PLOS PATHOGENS

RESEARCH ARTICLE

Foot-and-mouth disease virus localisation on follicular dendritic cells and sustained induction of neutralising antibodies is dependent on binding to complement receptors (CR2/CR1)

Lucy Gordon[1,2], **Neil Mabbott**[2], **Joanna Wells**[1], **Liudmila Kulik**[3], **Nick Juleff**[4], **Bryan Charleston**[1]*, **Eva Perez-Martin**[1]

1 The Pirbright Institute, Woking, United Kingdom, **2** The Roslin Institute and Royal (Dick) School of Veterinary Studies, University of Edinburgh, Edinburgh, United Kingdom, **3** Division of Rheumatology, Department of Medicine, University of Colorado School of Medicine, Aurora, Colorado, United States of America, **4** Bill and Melinda Gates Foundation, Seattle, Washington, United States of America

* bryan.charleston@pirbright.ac.uk

OPEN ACCESS

Citation: Gordon L, Mabbott N, Wells J, Kulik L, Juleff N, Charleston B, et al. (2022) Foot-and-mouth disease virus localisation on follicular dendritic cells and sustained induction of neutralising antibodies is dependent on binding to complement receptors (CR2/CR1). PLoS Pathog 18(5): e1009942. https://doi.org/10.1371/journal.ppat.1009942

Editor: Raffael Nachbagauer, Moderna Therapeutics Inc, UNITED STATES

Received: September 7, 2021

Accepted: April 12, 2022

Published: May 5, 2022

Data Availability Statement: All relevant data are within the manuscript and its Supporting Information files.

Funding: This work was supported by the Biotechnology and Biological Sciences Research Council (BBSRC). LG was funded by a PhD scholarship from R(D)SVS, University of Edinburgh and The Pirbright Institute. The Pirbright Institute receives strategic funding support from

Abstract

Previous studies have shown after the resolution of acute infection and viraemia, foot-and-mouth disease virus (FMDV) capsid proteins and/or genome are localised in the light zone of germinal centres of lymphoid tissue in cattle and African buffalo. The pattern of staining for FMDV proteins was consistent with the virus binding to follicular dendritic cells (FDCs). We have now demonstrated a similar pattern of FMDV protein staining in mouse spleens after acute infection and showed FMDV proteins are colocalised with FDCs. Blocking antigen binding to complement receptor type 2 and 1 (CR2/CR1) prior to infection with FMDV significantly reduced the detection of viral proteins on FDCs and FMDV genomic RNA in spleen samples. Blocking the receptors prior to infection also significantly reduced neutralising antibody titres, through significant reduction in their avidity to the FMDV capsid. Therefore, the binding of FMDV to FDCs and sustained induction of neutralising antibody responses are dependent on FMDV binding to CR2/CR1 in mice.

Author summary

Foot and mouth disease virus causes a highly contagious acute vesicular disease, resulting in more than 50% of cattle, regardless of vaccination status, and almost 100% of African buffalo becoming persistently infected for long periods (months) of time. Yet, the mechanisms associated with establishment of persistent infections are still poorly understood. Post infection, animals are characterised by the presence of long-lived neutralising antibody titres, which contrast with the short-lived response induced by vaccination. We have used a mouse model to understand how foot-and-mouth disease virus is trapped and retained in the spleen for up to 28 days post infection and how the absence of antigen on

BBSRC [BBS/E/I/00007032, BBS/E/I/00007037, BBS/E/I/00007039]. The Roslin Institute receives strategic funding support from BBSRC [BB/ BBS/E/D/20002174]. The funders had no role in study design, data collection and analysis, decision to publish, or preparation of the manuscript.

Competing interests: The authors have declared that no competing interests exist.

FDCs correlates with a reduced neutralising antibody response. Our results highlight the potential of targeting antigen to FDCs to stimulate potent neutralising antibody responses after vaccination.

Introduction

One of the features of foot-and-mouth disease virus (FMDV) infection, which has a major impact on the control and eradication of foot-and-mouth disease (FMD), is the existence of the "carrier state" [1,2]. A carrier of FMDV is defined as an animal from which live virus can be recovered from the nasopharynx after 28 days following infection, which frequently occurs in ruminants after acute infection [3]. Only ruminants have been shown to become FMDV carriers, and among them, the majority of infected African buffalo become carriers after acute infection and can carry FMDV for up to 5 years or more, which is why African buffalo are considered the primary reservoir of FMDV in Africa [4–7]. Over 50% of cattle exposed to FMDV become carriers [4,5,8], and although current vaccines prevent clinical disease, they do not prevent primary infection in the nasopharynx, therefore vaccinated animals can still become carriers of FMDV [9].

FMDV infection of ruminants elicits the production of specific serum neutralising antibodies which can provide protection for years [6,10]. T cell depletion studies in cattle identified that $CD4^+$ T-cell-independent antibody responses are required for resolution of clinical FMD in cattle [11]. Similarly, FMDV vaccines induce predominantly $CD4^+$ T-independent antibody responses that are enhanced by T cell activation [12]. Current inactivated FMD vaccines generally offer only a short-lived immune response in the host, due to the inability to induce FMDV-specific memory B cells. Neither infection nor vaccination induces a significant number of circulating memory B cells, despite a key difference of longer duration of immunity post-infection compared to post-vaccination [13].

Antigen retention on stromal follicular dendritic cells (FDCs) has been shown to maintain humoral immune responses by retaining antigen-containing complement-coated immune complexes (ICs) on their surface for long periods of time via complement receptors (CR2/CR1) and/or antibody Fc receptors [14–16]. FDCs are specialised immune cells of stromal origin found in the spleen, lymph nodes (LNs) and other lymphoid tissue including tonsil and mucosal surfaces, within B cell follicles in the light zones of germinal centres (GCs) [17]. They are necessary for GC formation, lymphoid follicle organisation and promoting B cell proliferation, survival and differentiation [18]. FDCs display native antigens within ICs to both naïve and GC B cells; therefore, FDCs are crucial for an effective humoral immune response [19]. The longevity of FDCs and their ability to trap and retain antigens in their native forms has also been exploited by certain pathogens. FDCs represent a major extracellular reservoir for a number of viruses and other pathogens including, but not limited to, human immunodeficiency virus (HIV), vesicular stomatitis virus (VSV), bovine viral diarrhoea virus (BVDV) and prions [20–23]. Juleff et al. first hypothesised that upon natural infection FMDV binds to and is retained by FDCs in the form of immune-complexed FMDV particles, resulting in prolonged stimulation of the anti-FMDV immune response, which maintain high levels of neutralising antibodies through continual exposure of B cells to FMDV-ICs on FDCs [24]. In cattle it was demonstrated that the virus can persist in association with FDCs in the lymphoid tissues of the head and neck [24]. These data provided insight into the potential mechanisms of viral persistence and the long-lasting antibody responses seen upon natural infection. An alternative study has described the site of FMDV persistence as pharyngeal epithelial cells in

both vaccinated and non-vaccinated persistently infected cattle within the mucosa-associated lymphoid tissue, interestingly associated with $CR2^+$ sub-epithelial lymphoid follicles [25]. Our previous data have also suggested that in buffalo persistently infected with the Southern African Territories (SAT) FMDV serotypes SAT-1, SAT-2 and SAT-3, quantities of FMDV RNA were significantly higher in the GC-containing regions of lymphoid tissues compared to epithelium samples, which again warranted further investigation into the possibility of virus-persistence in association with FDCs [26].

Data from experiments in mice have been fundamental in demonstrating the complement receptor-mediated retention of certain pathogens on FDCs [27,28]. For example, Ho et al. were able to demonstrate the binding of HIV to lymph node FDCs by using a rat monoclonal antibody (mAb) 7G6 to block CR2, which in turn prevented binding and retention of virions [29]. This observation was confirmed with the use of CR2/CR1-deficient ($Cr2^{-/-}$) mice, whereby no virus could be detected on FDCs [29].

Using a mouse model of FMDV persistence, our previous data suggested that splenic FDCs were able to trap and maintain FMDV for up to 63 days post infection (dpi) [30]. The main aim of the current study was to identify the receptor(s) involved in the maintenance of FMDV antigen within the spleen, and whether retention of antigen impacted the generation and maintenance of neutralising antibodies to FMDV in mice. We show that the blocking of CR2/CR1 on FDCs prevented binding and retention of FMDV, strongly suggesting this interaction is mediated by FMDV binding to CR2/CR1. Further investigation using super-resolution microscopy showed significant co-localisation of FMDV antigen with $CR2/CR1^+$ FDCs in the spleen. Moreover, blocking of CR2/CR1, and consequently absence of FMDV antigen on FDCs, resulted in the significant reduction of neutralising antibody responses to FMDV. A key function of FDCs in the GC reaction is the presentation of antigen, in the form of ICs, to B cells, driving affinity maturation. Blocking CR2/CR1 resulted in antibodies with a reduced capacity to neutralise virus and lower binding affinity to FMD virus-like particles (VLPs) compared to control animals. Until now, CR2/CR1 were not known to bind and maintain FMDV antigen on FDCs, or the impact of antigen retention on the production of high avidity, neutralising antibodies; therefore, knowledge of this interaction could enable a targeted approach to vaccine design, through the binding of complement-coated FMDV-ICs on FDCs via CR2/CR1 to increase duration of immunity post-vaccination.

Results

FMDV can only bind *ex vivo* to FDCs in the form of immune complexes

The binding of FMDV to the FDC network in spleen samples harvested from naïve mice was examined *in situ*. Spleen samples embedded in O.C.T compound from naïve mice were used to evaluate the ability of FMDV to bind in different forms. The three forms evaluated, all in the presence of complement provided through the addition of normal mouse serum (NMS), were: FMDV antibody (IB11) alone, FMDV antigen (O1/Manisa/TUR/69) alone and FMDV ICs (antibody and antigen). FMDV was only able to bind in clusters typical of FDC networks, as seen in spleen samples following *in vivo* FMDV infections in mice [31], when in the form of ICs. The negative control condition, IB11 FMDV antibody alone with NMS, produced no signal (Fig 1A) and only a small number of isolated cells were positive for FMDV upon addition of antigen alone with NMS (Fig 1B). A bright signal is detected when FMDV antigen, FMDV antibody and NMS have been incubated together for 1 hour, to allow formation of ICs, prior to addition to the spleen samples (Fig 1C).

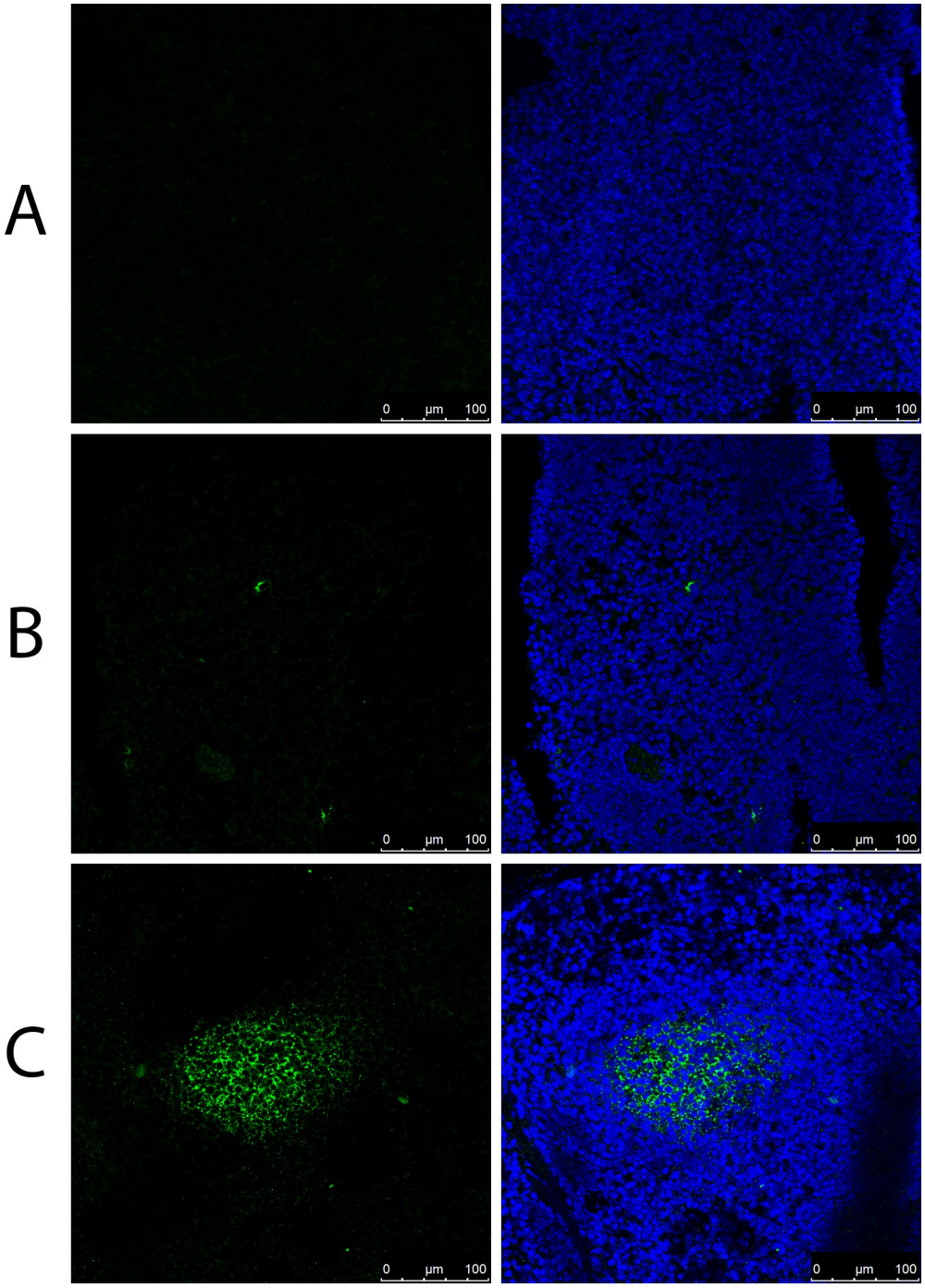

Fig 1. *Ex vivo* FMDV immune complex deposition assays. Confocal microscopy images of cryosections from naïve mice spleens after addition of different forms of FMDV. (A) FMDV antibody (IB11), (B) FMDV antigen (O1/Manisa/TUR/69) or (C) FMDV ICs (O1/Manisa/TUR/69 antigen and IB11 antibody) were pre-incubated for 1 hour with 5% NMS prior to addition to the cryosections. FMDV (green) was labelled with polyclonal rabbit anti-FMDV-O1 and detected using anti-rabbit 488. (A) Absence of signals for FMDV in spleen cryosections when treated with antibody alone, (B) few isolated cells stained positive for FMDV upon addition of antigen alone and (C) large bright green clusters showing the binding of FMDV ICs in the B cell follicles in the spleen. Nuclei stained blue (DAPI). Scale bars = 100µm.

https://doi.org/10.1371/journal.ppat.1009942.g001

Monoclonal antibody (mAb) 4B2 binds CR2/CR1^{+} in Balb/C mice and does not affect the proportion of immune cells in the spleen

In order to study antigen retention, a mouse anti-CR2/CR1 mAb 4B2 was used, which had been shown to block CR2/CR1 for up to 6 weeks *in vivo* in C57 Black mice, thus an excellent reagent for studying long term persistence of FMDV on FDCs in mice [32]. First, mice were injected with mAb 4B2, or IgG1 as an isotype control, and effects on splenocytes determined by flow cytometry at intervals afterwards up to 35 days post injection. We chose three anti-CR mAbs to test the blocking ability of mAb 4B2 up to 35 days post injection. The most notable reduction was the binding of mAb 7G6 to splenocytes from 2 days post inoculation (Fig 2A). This mAb binds a similar and overlapping epitope on CR1 and CR2 as mAb 4B2 as described previously [32].

Up to 35 days post inoculation mAb 4B2 is still capable of blocking CR, with a significant reduction of anti-CR2/CR1 mAbs binding to splenocytes, as demonstrated not only by mAb 7G6, but mAbs 8C12, which is monospecific to CR1, and 7E9, which binds a different epitope on CR2/CR1 (Fig 2B). This is in alignment with previous data, whereby the blocking effect is not purely due to steric inhibition, but induces a substantial decrease in the expression level of receptors when mAb 4B2 is used *in vivo* [32].

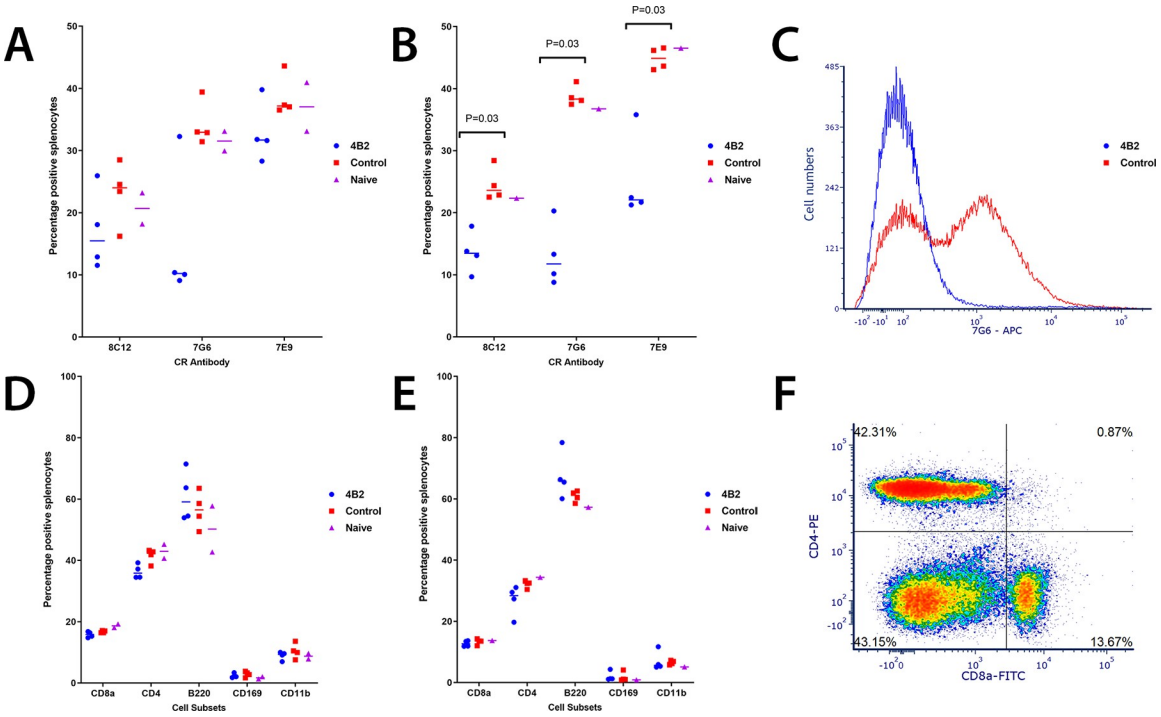

Fig 2. Flow cytometric analysis of splenocytes from mice treated with mAb 4B2 or control IgG, comparing cell subsets and availability of CR. Flow cytometry was used to identify the availability of complement receptors in mice after treatment with mAb 4B2 and the percentage of cell subsets, compared to control mice treated with IgG1. Spleen samples were taken at (**A**, **D**) early time points and (**B**, **E**) late time points from mice treated with 4B2 or IgG1 and naïve animals. At the early time points (**A**) there is a trend whereby mice treated with mAb 4B2 show a smaller number of positive cells to the CR antibodies, compared to the IgG1 or control groups, although this is not significant; 8C12 p = 0.312; 7G6 p = 0.061; 7E9 p = 0.194. By the late time points (**B**) mice treated with 4B2 had significantly reduced binding of the three anti-CR antibodies (p = 0.03) to their cells compared to the control mice. A representative histogram (**C**) of the number of cells positive for mAb 7G6 (CR2/CR1) from a mouse in the control group compared to a mouse from the mAb 4B2 treated group at the late time points. The percentage of the different splenic cell subsets CD8 and CD4 T cells, B cells (B220), macrophages (CD169) and dendritic cells (CD11b) (**D**-**E**) remained unchanged after treatment with 4B2 when analysed from both early and late time points after antibody treatment. A representative flow plot (**F**) of the CD8a and CD4 positive cells from a mouse from the 4B2 group at a late time point. Naïve animals were used as controls as they were untreated. *p values are 0.03 using the non-parametric Mann-Whitney U test to compare the medians of the two treatment groups.

https://doi.org/10.1371/journal.ppat.1009942.g002

Treatment with mAb 4B2 did not affect the abundance of CD8a cytotoxic T cells, CD4 T helper cells, B cells (B220+ cells), marginal zone macrophages (CD169) and monocytes (CD11b), at early or late timepoints (Fig 2D and 2E respectively). Importantly, immunohistochemistry (IHC) analysis showed the presence of CD21/CD35+ FDCs in the spleens of mice treated with mAb 4B2 (Fig 3). These data are consistent with data from Kulik et al. that also reported that i*n vivo* injection of mAb 4B2 does not induce the death of immune cells including FDCs, but leads to substantial blocking of binding of other mAb to CR2 and CR1 [32].

Reduced immune complex trapping by FDC in the spleens of mice treated with mAb 4B2

We next investigated the effects of *in vivo* mAb 4B2 treatment on the ability of FDCs to trap ICs. Mice were injected with mAb 4B2 (or an IgG1 isotype control) and 1 day later injected with pre-formed peroxidase-anti-peroxidase (PAP) containing ICs which can bind to FDCs *in vivo* via CR2/CR1 [33]. Spleen sections were analysed by confocal microscopy 1 day later (Fig 3). The presence of CR2/CR1-expressing FDC was detected using mAb 7E9. In control-treated mice, PAP-ICs were consistently detected in association with FDC networks, with 95% of the FDC networks positive for PAP. In contrast, in the spleens of mice treated with mAb 4B2, PAP-ICs were detected in fewer than 2% of the FDC networks examined, similar to the background levels observed in naïve mice (Table 1). This data demonstrates that pre-treatment of mice with mAb 4B2 effectively blocks the retention of ICs by splenic FDCs *in vivo*.

CR2/CR1-blockade enhances the viraemia during FMDV infection

Next, we determined the effects of mAb 4B2-mediated CR2/CR1-blockade on the viraemia during FMDV infection. Mice were treated with mAb 4B2, or IgG1 as a control, and 1 day later injected with FMDV. By two days after infection a statistically significant, 10-fold increase in the viraemia in sera was detected in mAb 4B2-treated mice compared to control-treated mice (Fig 4A). Viral RNA quantification corroborated the plaque assay results, whereby mAb 4B2-treated mice showed a statistically significant, 10-fold increase of viral genome in the serum compared to the control-treated mice (Fig 4B). By 7 dpi the viraemia was cleared in both groups and no detectable virus was detected by plaque assay or qPCR. Naïve mice were used as negative controls and were negative for both the plaque assay and qPCR. These data importantly show that blockade of CR2/CR1 did not affect the ability of the virus to replicate, in fact the CR2/CR1 blockade resulted in a higher titre of virus in sera post-infection with FMDV in mice.

CR2/CR1-blockade reduces the trapping and persistence of FDMV antigen in the spleen

Next, we determined whether CR2/CR1 blockade similarly impeded the trapping and persistence of FMDV in the spleen. Mice were treated with mAb 4B2 or IgG1, 1 day later injected with FMDV, and spleens (n = 8/group) collected at weekly intervals afterwards. Spleens from naïve mice were used as controls. The location of FMDV and FDC networks in the spleens was determined by immunofluorescence confocal microscopy (Fig 5A–5D). We used mAb 7E9 to detect FDC since the treatment of mice with mAb 4B2 does not completely block the binding of mAb 7E9 to CR2/CR1 (Figs 2 and 3). The total number of FDC networks and whether they were positive or negative for FMDV is represented in Table 2.

Despite the differences in FMDV antigen retention on FDCs, the total number of FDCs from mice in both the IgG1 control group and the mice treated with the CR2/CR1-blockade

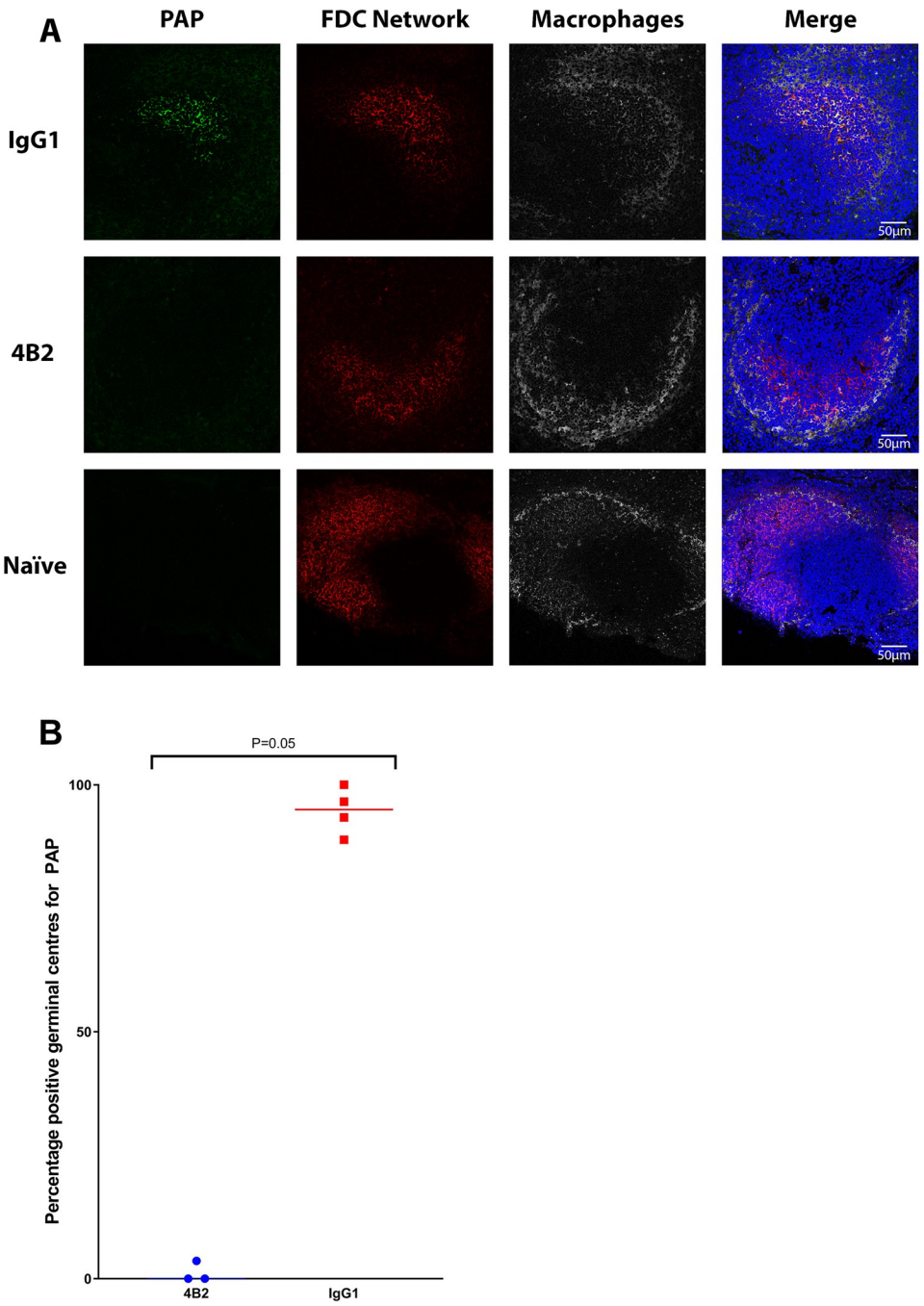

Fig 3. Effect of pre-treatment with mAb 4B2 on the binding of PAP on the FDC networks in mouse spleen. BALB/c mice were treated with 500 μg of 4B2 (n = 3) or IgG1 (n = 4) control 24 hours before immunisation intravenously with peroxidase anti-peroxidase (PAP). Naïve mice were untreated. Spleen samples were collected in OCT compound from mice culled 1-day post inoculation with PAP. **A**) Cryosections were analysed via confocal microscopy for the presence of PAP associated to the FDC network. Confocal microscopy images are arranged in rows and columns according to the treatment and the staining. **B**) Mice from the 4B2 treatment group had significantly less PAP bound to FDCs compared the control group, p value of 0.05 using the non-parametric Mann-Whitney U test to compare the medians of the two treatment groups. **PAP panels**: show PAP labelled green, detected with anti-rabbit 488. PAP was detected in FDC networks in IgG1 control mice, but not in 4B2 treated mice. Absence of signal to PAP in naïve mouse spleen. **FDC Network**: light zone FDCs labelled red with Alexa Fluor 594-conjugated anti-mouse CD21/CD35 (CR2/CR1) antibody, clone 7E9; FDC clusters were detected in all groups. **Macrophages**: marginal zone macrophages surrounding the light zone GC labelled grey with conjugated mAb CD169-APC. **Merged images**: show deposition of PAP within the FDCs network (yellow, co-localisation) of the IgG1 control mice but not in 4B2 treated mice or naïve mice. Nuclei stained blue (DAPI). Scale bars = 50 μm.

https://doi.org/10.1371/journal.ppat.1009942.g003

Table 1. Immunofluorescence examination of FDC networks in spleens of mice treated with CR block (4B2) or an isotype control (IgG1) 1 day before PAP immunisation.

Groups	4B2[a]	IgG1[b]
Total number of FDC networks imaged	128	166
Number of FDC networks positive for PAP	2	158
Percentage of FDC networks positive for PAP (%)	1.6	95.2
Medians of PAP-positive FDC networks	0.00	95

[a]n = 3 mice

[b]n = 4 mice

https://doi.org/10.1371/journal.ppat.1009942.t001

were not significantly different (Fig 6A). This confirms data obtained previously [32], and therefore the significant reduction in FMDV antigen retention in mice pre-treated with mAb 4B2 is not due to the lack of FDC networks, but specifically as a result of the blockade of CR2/CR1.

In IgG1 isotype control treated mice, FMDV antigen was detected in the majority of FDC networks by 7 dpi. Although the number of FMDV-antigen-positive FDC networks gradually declined as the infection progressed, FMDV antigen was detectable in association with approximately 10% of the FDC networks at 28 dpi (Fig 6B). In contrast, no association of FMDV antigen with FDCs above background levels was detected in the spleens of mAb 4B2 treated mice, with the exception of 4 mice, suggesting that CR2/CR1-blockade had prevented the trapping and retention of FMDV on FDC.

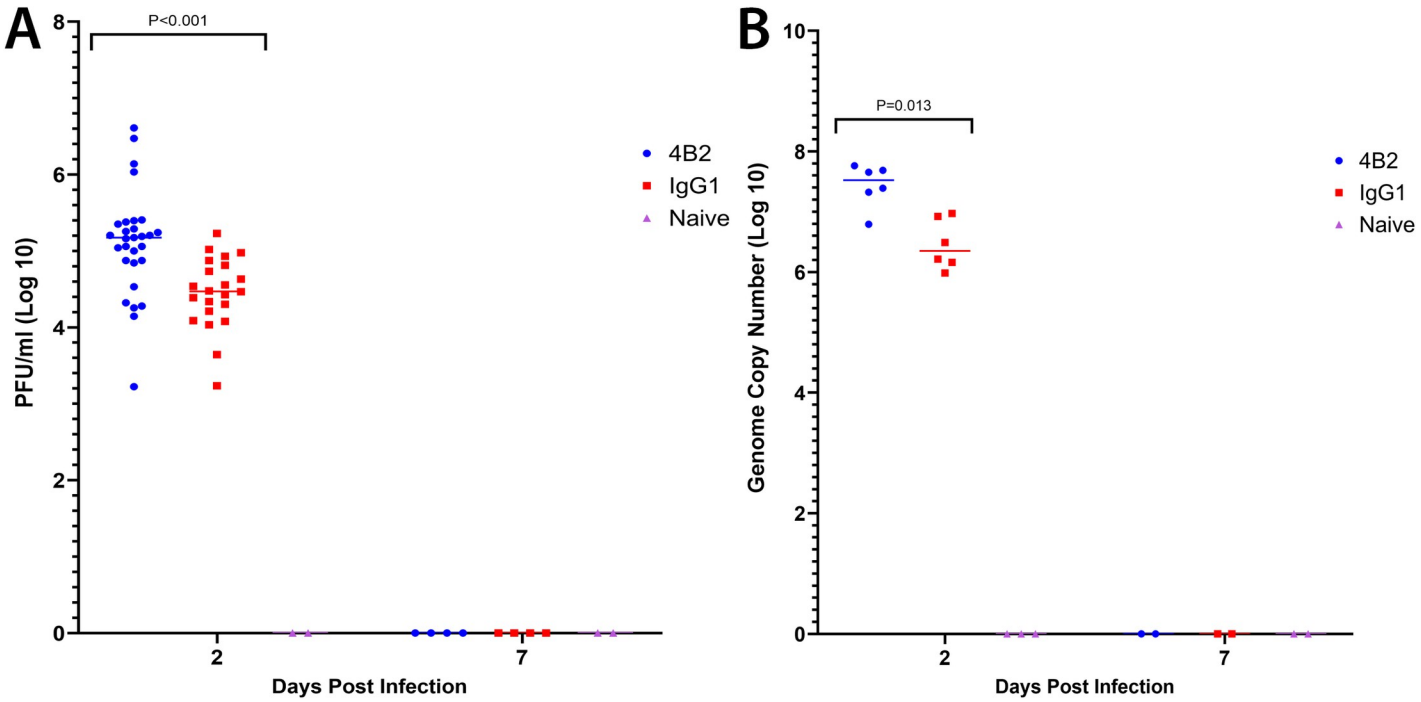

Fig 4. Viraemia in 4B2 treated and control-treated mice in response to FMDV infection. The presence of viraemia in serum samples from mice treated with 4B2 or IgG1 was investigated by (**A**) plaque assay and (**B**) qRT-PCR. Serum samples were collected from 4B2 and IgG1 treated mice at 2 and 7 dpi. The quantity of virus in the mouse serum at 2 dpi is expressed as (**A**) log 10 of the number of plaque forming units (PFU) per 1 ml serum and (**B**) log 10 of the genome copy number (GCN), with CT values $\geq$ 35 for 3D FMDV deemed negative and recorded as 0. Each data point represents an individual animal, and the line represents the median values. Naïve mice at 2 dpi and all serum samples harvested from 7 dpi were negative for viraemia. P values of <0.05 using the non-parametric Mann-Whitney U test to compare the medians of the two treatment groups.

https://doi.org/10.1371/journal.ppat.1009942.g004

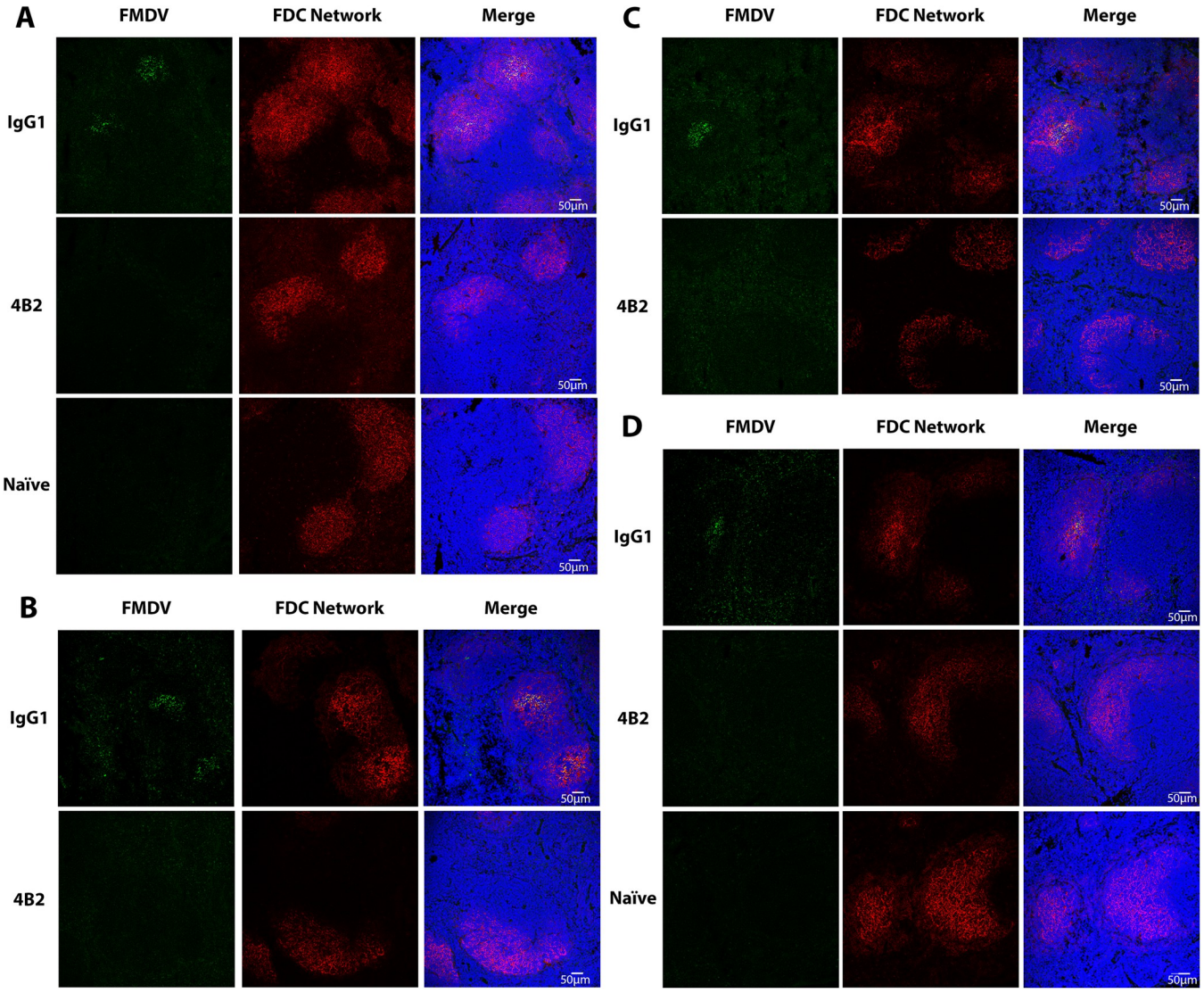

Fig 5. Effect of pre-treatment with 4B2 preventing the binding of FMDV on FDCs in mouse spleens. Confocal microscopy images are arranged in rows and columns according to the treatment, day post infection and the staining. BALB/c mice treated with 500 μg of either mAb 4B2 or IgG1 control on day -1 before challenge with FMDV. FMDV-infected mouse spleen samples were collected at (**A**) 7, (**B**) 14, (**C**) 21 and (**D**) 28 dpi from IgG1 control mice and 4B2 mice (n = 8 per group per timepoint). Naïve mouse spleens were taken at 7 dpi (n = 4) and 28 dpi (n = 4). **FMDV panels**: show FMDV protein labelled green with biotinylated llama single domain anti-FMDV 12S antibody VHH-M3 and streptavidin Alexa-Fluor-488. FMDV was detected in the IgG1 control group at all timepoints. FMDV was not detected in the spleens of the 4B2 treated group at any of the time points, with the exception of four mice, three harvested at day 14 and one at day 21. There was an absence of signal for FMDV in naïve mouse spleen at all time points. **FDC Network**: show FDCs labelled red with Alexa Fluor 594-conjugated anti-mouse CD21/CD35 (CR2/CR1) antibody, clone 7E9; FDC clusters were detected at all time points in control, 4B2 treated and naïve mice. **Merged images**: show deposition of FMDV within the light zone FDC network of IgG1 control mice (yellow–colocalization); but absence of FMDV within the light zone FDC network of 4B2 treated mice and naïve mice (red). Nuclei stained blue (DAPI). Scale bars = 50 μm.

https://doi.org/10.1371/journal.ppat.1009942.g005

Comparison of the presence of viral RNA similarly revealed that CR2/CR1-blockade had prevented the accumulation and persistence of FMDV in the spleen. While high levels of viral RNA were detected in the spleens of control-treated mice until 21 dpi, the levels in 4B2-treated mice were below the detection limit (Fig 6C). However, although FMDV antigen was detectable in association with FDCs in the spleens of control-treated mice by 28 dpi, the levels of viral RNA in whole spleen samples were below the detection limit in all groups at this time. Thus, these data show that trapping and persistence of FMDV antigen is dependent on FMDV binding to FDCs via CR2/CR1.

Table 2. Immunofluorescence examination of mouse spleen treated with mAb 4B2 or control IgG1 for FMDV in FDC networks at 7, 14, 21 and 28 dpi and naïve mice at 7 and 28 dpi.

Groups	4B2[a]				IgG1[a]				Naïve[b]	
DPI	7	14	21	28	7	14	21	28	7	28
Number of FDC networks	579	1078	1100	1091	549	1106	1146	1236[T]	244	575
Number of FDC networks positive for FMDV	10	152	18	3	343	357	258	128	5	10
Percentage FDC networks positive for FMDV (%)	1.73	14.1	1.6	0.3	62.5	32.3	22.5	10.4	2.05	1.7
Medians of FDC networks positive for FMDV	0.83	0.31	0.96	0.00	63.09	32.97	22.64	9.11	1.89	1.76

[a]n = 8 mice per time point

[b]n = 4 mice per time point

https://doi.org/10.1371/journal.ppat.1009942.t002

Co-localisation of CR2/CR1 with FMDV

Localisation of FMDV was consistently found in murine spleens within the FDC networks. Further investigation using stimulated emission depletion (STED) microscopy for super-resolution images confirmed that FMDV proteins were predominantly co-localised with CR2/CR1 on FDCs (Fig 7). ImageJ software was used to confirm that the distribution of the CR2/CR1- and FMDV-antigen-associated fluorochromes were preferentially co-localised, compared to that predicted by the null hypothesis that each of these were randomly and independently distributed [33,34]. This analysis confirmed a highly significant and preferential association of the FMDV antigen with CR2/CR1 on FDCs when compared to the null hypothesis that the pixels were randomly distributed (Fig 7B).

Virus isolation

In order to determine whether the FMDV antigen retained on the FDCs in murine spleens was infectious, an FMDV-susceptible cell line was inoculated with spleen homogenates from FMDV infected animals. The spleens from 7 mice culled at 7 dpi were used: 2 mice pre-treated with the mAb 4B2; 2 mice pre-treated with the IgG1 isotype control and 3 mice which received no prior treatment before infection with FMDV. All samples were negative confirming previous reports, that in the mouse model [31], infectious FMDV could not be detected in whole spleen samples even though antigen could be detected in the FDC networks.

CR2/CR1-blockade reduces the generation of neutralising antibodies in FMDV infected mice

Since the retention of antigen on FDCs is important for the induction and maintenance of high-titre antibody responses and B cell affinity maturation [14,35], we next tested the hypothesis that CR2/CR1-blockade in FMDV-infected mice would impede the generation of virus neutralising antibodies. Serum samples were collected from mAb 4B2- or control IgG1-treated FMDV-infected mice and incubated with FMDV-susceptible cells and FMDV for their ability to neutralise the virus.

High titres of virus-specific neutralising antibodies were detected in the sera of control IgG1-treated mice by 7 dpi, titres increased by day 14 and these were maintained up to 28 dpi (Fig 8). In contrast, while virus-specific neutralising antibodies were detected in the sera of mAb 4B2-treated mice by 7 dpi, these did not increase at later time points post infection and their titres were significantly reduced when compared to those in the serum of control IgG1--treated mice (Fig 8).

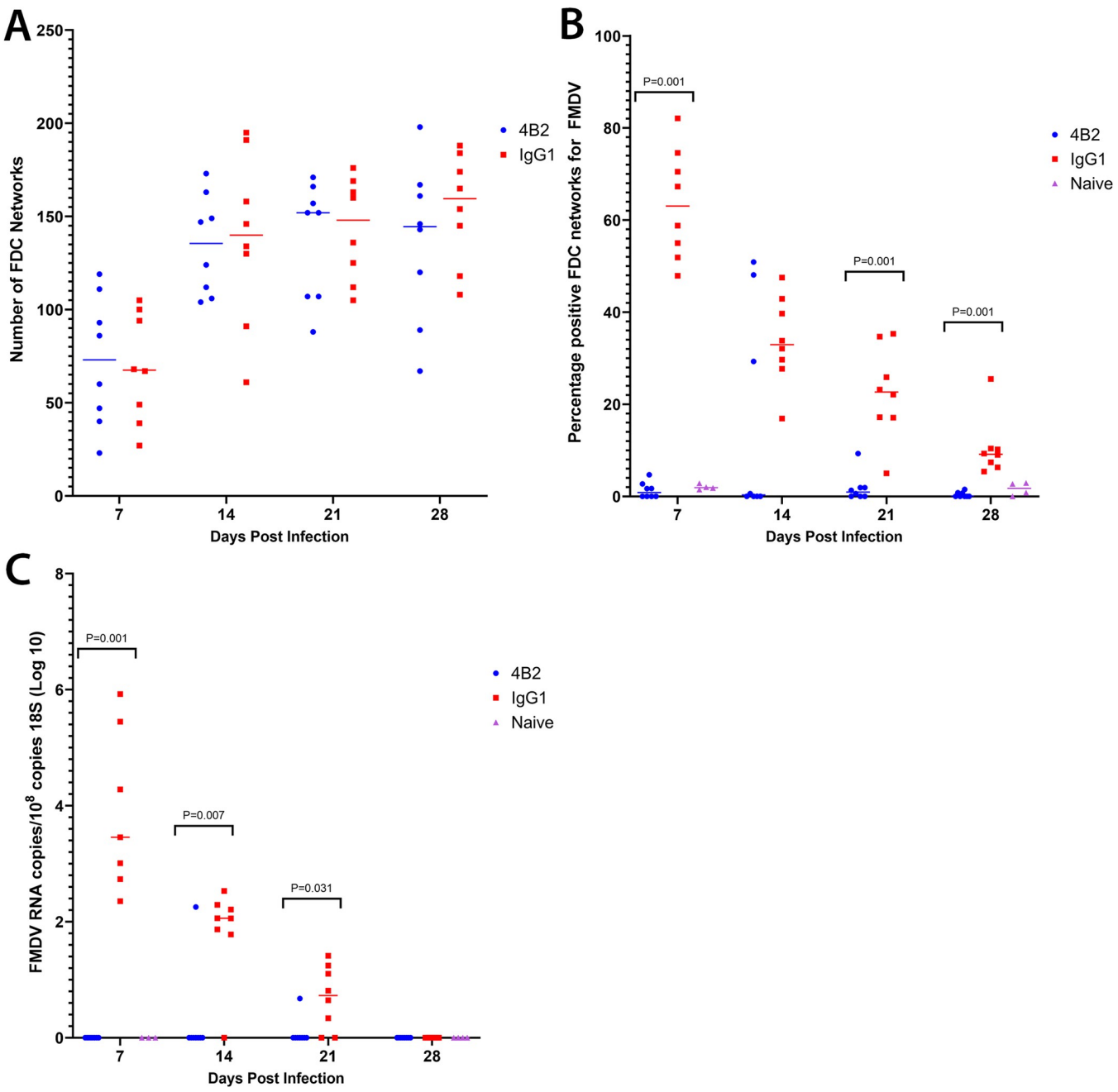

Fig 6. Quantification of FMDV antigen and RNA in spleens from 4B2-treated and isotype control treated mice detected by confocal microscopy and RT-qPCR. Spleen samples were collected from BALB/c mice at 7, 14, 21 and 28 dpi (n = 8/group/timepoint) following treatment with either mAb 4B2 or IgG1 isotype control one day prior to IP challenge with $10^{6.2}$ $TCID_{50}$ of FMDV/O/UKG/34/2001.Sections were cut using a cryostat and a cross-section was taken of the spleens by consistently collecting 16 sections per animal with an approximate 70 μm gap between each section. **A**) FDC networks were visualised, imaged and counted using mAb 7E9, an anti-CR2/CR1 antibody. There were no significant differences in the total number of FDC networks in the group treated with mAb 4B2 compared to the IgG1 isotype control. **B**) FMDV was detected using a biotinylated llama single domain anti-FMDV 12S antibody VHH-M3, and the percentage of FDC networks which were positive for FMDV was calculated. Mice treated with mAb 4B2 had significantly less FMDV in their FDC networks compared to the isotype control mAb, with a P value of $\leq$0.001 from 7, 21 and 28 post infection. **C**) The samples were analysed by RT-qPCR for the presence of FMDV RNA and the results are expressed as copies per 10^8 copies of 18S rRNA. Each data point represents an individual animal, and the line represents the median values. CT values $\geq$ 35 for 3D FMDV were deemed negative and recorded as 0. Naïve mice (n = 4) were tested at 7 and 28 dpi as negative controls. Using the non-parametric Mann-Whitney *U* test to compare the medians of the two groups, at 7 dpi p value of 0.001; 14 dpi p value of 0.007; 21 dpi p value of 0.031.

https://doi.org/10.1371/journal.ppat.1009942.g006

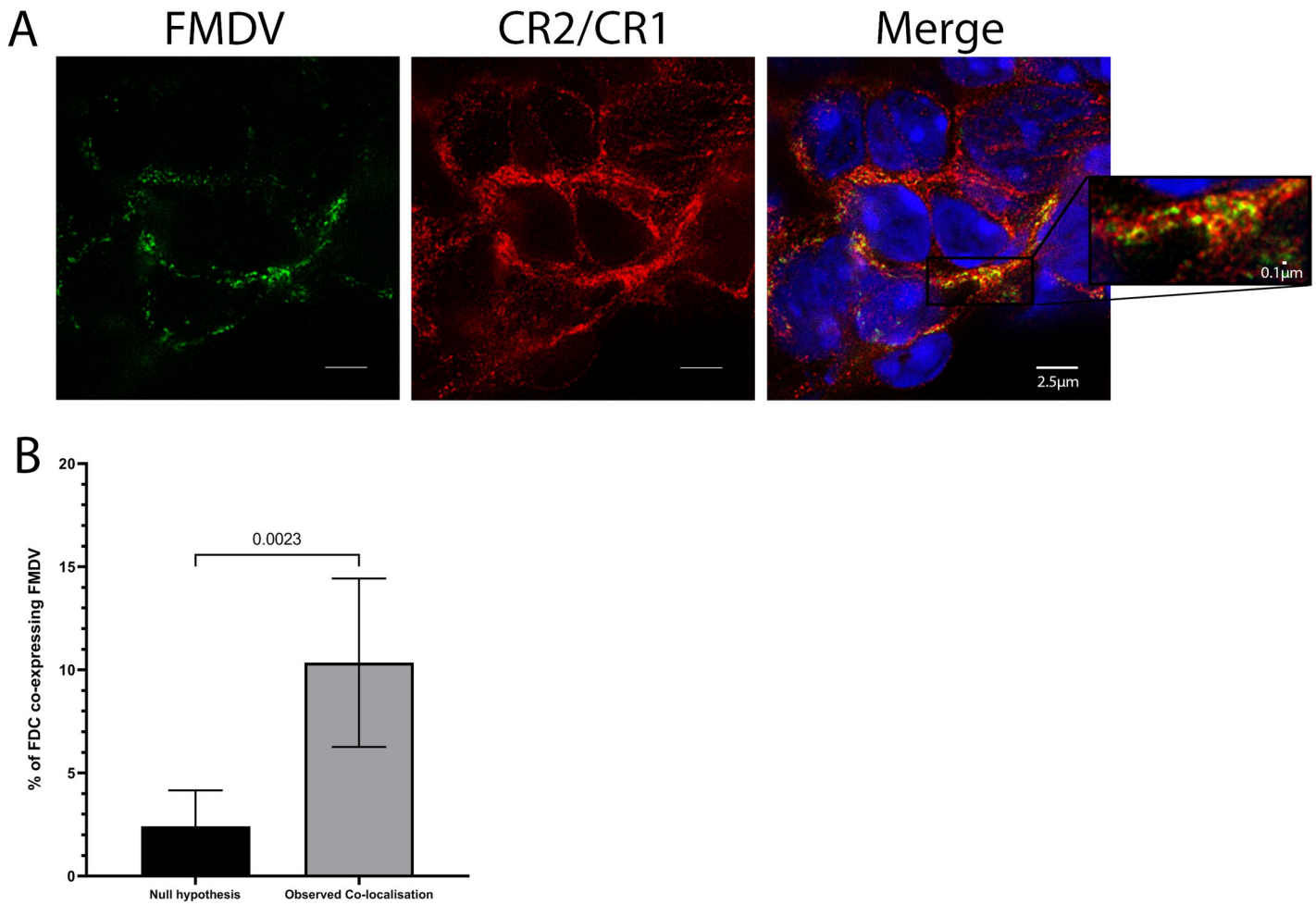

Fig 7. Co-localisation of FMDV with FDCs. BALB/c mice were infected with FMDV/O/UKG/34/2001 and high-resolution images were taken of spleen samples using a STED confocal microscope. **A**) Spleen taken from an infected mouse 7 dpi, demonstrating the co-localisation of FMDV (green) with FDCs (red). **B**) Morphometric analysis using ImageJ confirmed that FMDV was preferentially associated with FDCs in spleen tissues (n = 7) and significantly greater than the null hypothesis that the pixels were randomly distributed, with a p value of 0.0023.

https://doi.org/10.1371/journal.ppat.1009942.g007

CR2/CR1-blockade had no effect on the total IgG/IgM FMDV-specific antibody titres

We next used indirect ELISAs to determine the isotypes of the FMDV-specific antibodies produced in the sera of mice from each treatment group. Despite the significant decrease in the level of virus-neutralising antibodies in the sera of the mAb 4B2-treated mice, there were no significant differences in the titre of virus-specific IgG produced at any of the time points analysed (Fig 9A). A FMDV mAb of known concentration was used in the ELISA as a standard to determine the concentration of FMDV-specific IgG in the polyclonal sera (Fig 9B). At 7 dpi, 4 mice from the 4B2 group and 3 mice from the IgG1 group had FMDV-specific IgM antibodies, and as expected no mice had IgM titres after this timepoint (Fig 9C).

CR2/CR1-blockade reduces antibody titres to the neutralising FMDV G-H loop

Next, an ELISA was carried out to compare the antibody titres in the mAb 4B2-treatment group and the control group against the O/UKG/12/2001 $VP1_{129\text{-}169}$ G-H loop (Fig 10A). In

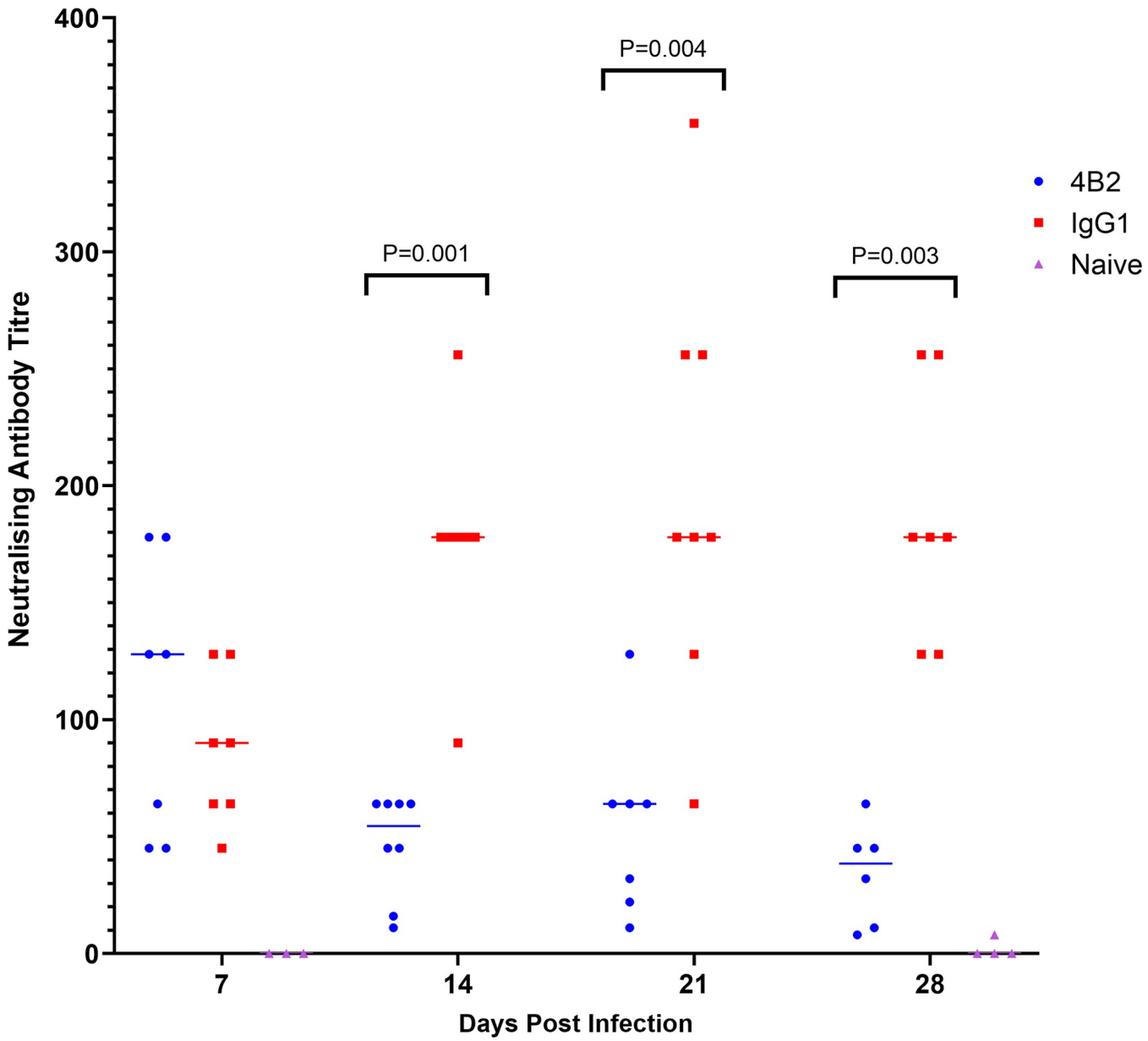

Fig 8. Effect of 4B2 treatment on titres of FMDV neutralising antibodies in mouse serum. FMDV neutralising antibodies were evaluated from serum samples taken from BALB/c mice at 7, 14, 21 and 28 dpi with FMDV. Mice had either been pre-treated with mAbs 4B2 or IgG1 1 day prior to FMDV infection. Naïve mice were used as controls. Each data point represents an individual animal, and the line represents the median antibody titre. Neutralising antibody titres are expressed as the serum dilution that neutralised 50% of 100 $TCID_{50}$ of the virus. Using the non-parametric Mann-Whitney *U* test to compare the medians of the two groups, at 14 dpi p value of 0.001, 21 dpi p value of 0.004 and 28 dpi p value of 0.003.

https://doi.org/10.1371/journal.ppat.1009942.g008

mice, the G-H loop is a neutralising epitope of FMDV, and a G-H loop peptide vaccine is sufficient to protect against FMDV challenge [36,37]. Mice treated with mAb 4B2 had significantly lower antibody titres to the G-H loop compared to the control group, which may have contributed to the decreased ability of the antibodies from the 4B2-treated mice to neutralise FMDV. However, addition of G-H loop peptide to inhibit the G-H loop activity in mouse sera did not significantly reduce the titre of the VNT assays; therefore, virus neutralisation is not solely conferred by binding to the GH-loop.

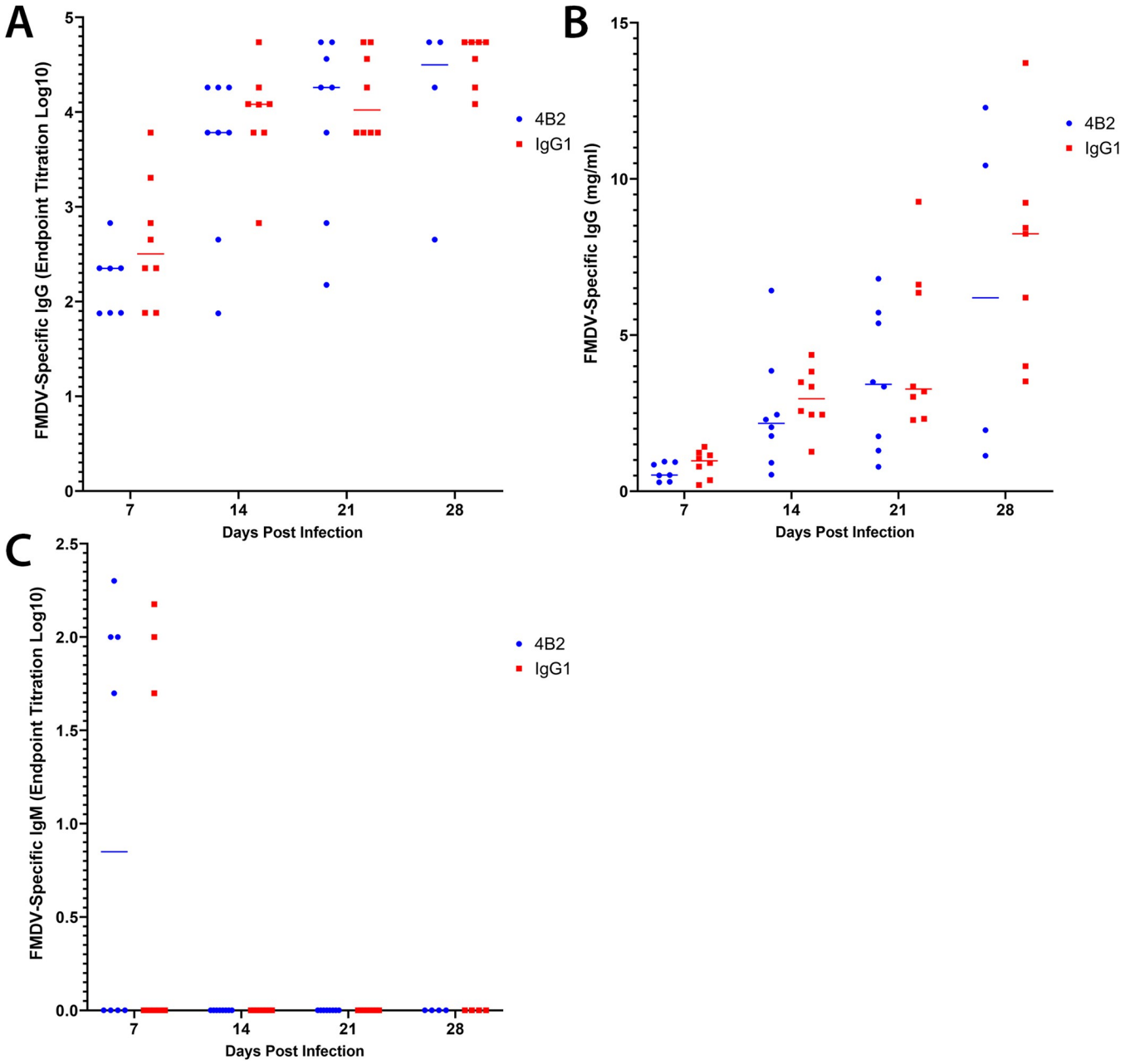

Fig 9. Effect of 4B2 treatment on titres of FMDV specific antibodies. FMDV-specific antibodies in serum samples from mice treated with mAb 4B2 or an isotype control antibody (IgG1) were detected by ELISA. Serum samples were collected at 7, 14, 21 and 28 dpi and tested for (**A**, **B**) IgG and (**C**) IgM antibodies. Naïve sera were included on all ELISA plates and the cut-off was set at 1.5 times the OD of the naïve sera. Antibody titres were either expressed as (**A**, **C**) the reciprocal log10 of the last positive dilution or (**B**) using a known FMDV IgG standard to plot the concentration of IgG antibodies in mg/ml. Each data point represents an individual animal, and the bars represent median values. Using the non-parametric Mann-Whitney *U* test to compare the medians of the two groups, there were no statistically significant differences at any time points.

https://doi.org/10.1371/journal.ppat.1009942.g009

CR2/CR1-blockade decreases antibody avidity to FMD VLPs

We then investigated whether CR2/CR1-blockade had affected the avidity of the FMDV-specific antibodies for FMDV antigen (Fig 10B). Using the data shown in Fig 9B, known concentrations of FMDV-specific IgG in polyclonal sera from infected mice from each group were incubated with stable FMD VLP and the antibody dissociation/association rates (k_{off}/k_{on}) rates

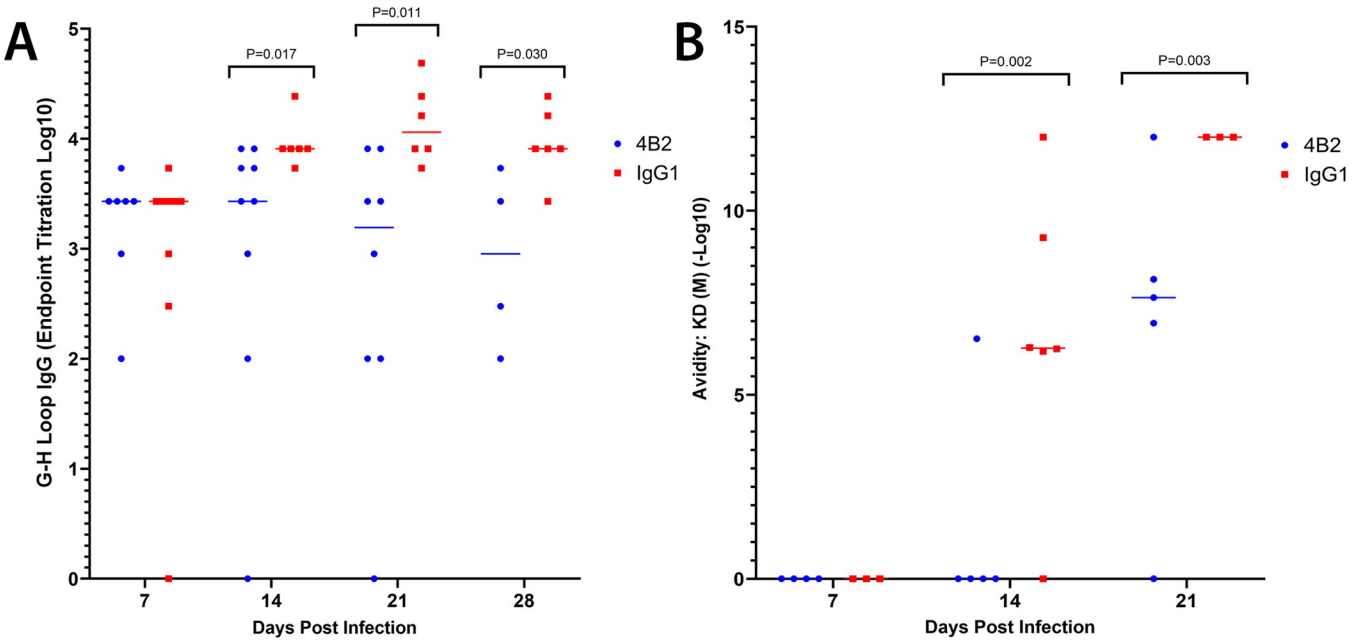

Fig 10. Effect of 4B2 treatment on titres of IgG antibodies specific to the FMDV G-H loop and the avidity of FMDV specific IgG antibodies in mouse serum. BALB/c mice treated with 500 μg of either mAb 4B2 or IgG1 control on day -1 before challenge with FMDV and sera was collected at 7, 14, 21 and 28 dpi. **A**) An indirect peptide ELISA showed that mice treated with 4B2 had significantly less antibodies to the FMDV G-H loop compared to the IgG1 control group, with a P value of ≤0.05 using the non-parametric Mann-Whitney *U* test. Naïve sera were included on all ELISA plates and the cut-off was set at 1.5 times the OD of the naïve sera. **B**) The avidity of antibodies was measured using biolayer interferometry and was performed using an Octet Red96e. FMD O1/Manisa/TUR/69 VLP were bound to streptavidin sensors and dipped into three dilutions of sera per mouse. Each data point represents the mean avidity of these measurements for each individual mouse, represented as -Log10 of the KD (M) value. Sera which produced a negative response rate, and therefore had too few antibodies bound to FMD VLPs to reach the limit of detection, are recorded as 0. The results demonstrate that mice treated with 4B2 had significantly lower avidity antibodies compared to the control group, with a P value of ≤0.05 using the non-parametric Mann-Whitney *U* test.

https://doi.org/10.1371/journal.ppat.1009942.g010

and K_D values determined. The K_D is the equilibrium dissociation constant between an antibody and its antigen and is measured using the ratio of k_{off}/k_{on}, therefore K_D values were used to represent the avidity of the polyclonal antibodies, based on the individual affinities of the antibodies in the polyclonal serum samples, to the FMD VLP. These data clearly showed that the K_D values in the sera of mice treated with mAb 4B2 were significantly lower than those in the sera of IgG1-treated control mice (Fig 10B); suggesting that virus-specific antibodies induced after CR2/CR1-blockade had reduced avidity to FMD VLP. This decrease in antibody avidity to the FMD capsid is likely the predominant cause of the reduced capacity of the antibodies generated after the CR2/CR1 blockade to neutralise FMDV, when compared to the control animals (Fig 8).

Discussion

Our previous studies suggested that in cattle FMDV is localised on FDCs in the B cell follicles [24]. Similar to studies with HIV where the interaction of virus with FDCs has been explored in detail in mice, we have demonstrated FMDV localises to FDCs in mice after the resolution of viraemia. The mouse model for FMDV persistence showed FMDV antigen retention in the spleen in association with FDC for up to 63 dpi [31]. We have now used this FMDV mouse model to gain novel insight into the mechanisms of FMDV persistence on FDCs. In this study, FMDV protein was detected in FDC networks up to 28 dpi and FMDV genome up to 21 days in spleen samples. We suspect the absence of detectable genome at 28 days is because the RNA will be in a small number of localised deposits in association with the FDC which may not be

detected when the whole spleen is sampled. We have shown previously in cattle and African buffalo that FMDV genome does persist in the GC-containing regions of infected lymphoid tissues for prolonged periods [24,26].

The absence of FMDV antigen and genome by IHC and PCR in mice treated with mAb 4B2 as reported here, demonstrates the role of CR2/CR1 as the major receptor involved in the trapping and retention of FMDV. Our data demonstrating no loss in viraemia is an important observation to show that the mAb 4B2 does not prevent viral replication, and therefore is not the reason for the lack of FMDV detection on the FDC networks in the animals treated with the CR2/CR1 blockade. In fact, our results showed that this blockade increased viraemia in these mice, and although we are not certain why, one hypothesis is that virus was unable to be cleared from the blood as effectively when CR2/CR1 was blocked.

Furthermore, blocking of CR2/CR1 results in a significant reduction of neutralising antibody titres against FMDV. Although two mechanisms have been described for antigen trapping by FDC, CR mediated [15] and FcR mediated [38], the near complete elimination of FMDV on FDCs after treatment with mAb 4B2 leads us to believe the trapping is predominantly CR2/CR1-dependent. However, we do not exclude that longer persistence of the virus on FDCs after natural infections, when anti-virus antibody forms, are due to a combination of FcR and CR2/CR1 binding.

Ochsenbein et al. used *Cr2*$^{-/-}$ mice to investigate antibody responses to a T-independent antigen, VSV. They showed similar findings, that early antibody responses to infection were unaffected in these knockout mice, including no significant effect on the IgM response to infection in mice deficient in CR2/CR1. However, longer term antibody responses to VSV were not significantly different in *Cr2*$^{-/-}$ mice compared to the wild type (WT) [39]. Unlike FMDV [13], VSV is able to induce B cell memory, therefore, the contrast to our findings could be because the induction of antibody responses to VSV are less dependent on antigen persistence on FDCs compared to FMDV. The murine *Cr2* gene encodes two proteins, CR1 and CR2, via alternative splicing [40], therefore inactivation of the *Cr2* gene leads to deficiency in both CR1 and CR2. The similarity in these receptors also leads to blocking of both CR1 and CR2 upon administration of an anti-CR2 and/or -CR1 mAb.

Cr2$^{-/-}$ mice have abnormalities in the maturation of GCs including the GC B cells associated with the CR2/CR1 deficiency, which may complicate the interpretation of some studies where they are used. These *Cr2*$^{-/-}$ mice have been shown in multiple studies to have a discernible impairment in their ability to mount a humoral immune response [41,42]. A recent study by Anania et al. used image analysis to demonstrate that FDCs lacking CR1 and CR2 not only have a decreased ability to capture ICs, but in the *Cr2*$^{-/-}$ mice, GCs are fewer and smaller and FDCs are poorly organised [43]. FDCs use chemokine gradients within the B cell follicles to interact with B cells and T follicular helper, therefore disorganisation of the FDC networks leads to a variety of abnormalities, including impaired B cell survival and reduced Ig production [44].

Although *Cr2*$^{-/-}$ mice are unable to mount a normal humoral immune response to various antigens, a study showed that *Cr2*$^{-/-}$ mice had reportedly normal levels of total IgM and of the different IgG isotypes, showing no evidence of altered B- or T- cell development [42]. These studies showed antibody titres were similar in *Cr2*$^{-/-}$ and WT mice, however functional differences in antibodies were not specifically investigated. We also showed IgM and IgG titres were similar in treated and control mice, but went on to show low avidity, non-neutralising antibodies were produced which could be due to a defective affinity maturation process due to the lack of binding of FMDV proteins to CR2/CR1 on FDCs. Furthermore, it has been established that in mice the G-H loop is a neutralising epitope inducing protection against FMDV [36]; and mice treated with mAb 4B2 had a modest reduction of antibodies to the G-H loop. These

results correlate with the reduced ability of the antibodies from the mice treated with 4B2 to neutralise FMDV from 7 dpi, although the reduction in avidity of the FMDV-specific antibodies appears to be the predominant reason for the differences in the virus neutralisation between the 2 groups.

Due to the off-target effects from using $Cr2^{-/-}$ knockout mice to study the function of FMDV antigen on FDC, we used the mAb 4B2 to block CR2/CR1 on FDCs. This antibody had been previously described to block these receptors for up to 6 weeks *in vivo* in mice, without disrupting other cell types. Bioimaging and flow cytometry analysis confirmed that the number and size of FDC networks were normal, and the percentage of other immune cell subsets in the spleen, including B- and T- cells were unaltered after blocking up to 35 days. We were therefore confident that the mAb 4B2 treatment would indicate whether antigen bound to CR2/CR1 on FDCs impacted on the immune response.

A number of studies have used $Cr2^{-/-}$ mice reconstituted with $Cr2^{+/+}$ WT bone marrow (BM) to allow a more specific investigation of the role of CR2/CR1 on FDCs without impairing B cell functions [45–47]. This is possible because FDCs are derived from stromal cells, whereas B cells are BM in origin. Initial IgG and IgM responses were shown to be similar in $Cr2^{-/-}$ mice with or without WT BM ($Cr2^{+/+}$ B cells), suggesting antigen can induce a B cell response in the absence of CR expression [45,46]. However, studies investigating the long-term antibody response of these chimeric mice have shown a significant reduction in both long-term antibody production and memory when FDCs specifically did not express *Cr2* [46,47]. This is in line with our results where neutralising antibody responses up to day 7 post infection were similar in mice with or without a CR2/CR1 block, yet after this timepoint, there was a significant reduction in FMDV neutralising antibodies in mice treated with the anti-CR2/CR1 mAb.

It is well established that CR1 and CR2 are essential for binding ICs and are expressed at high levels on FDCs; and while FDCs can also trap ICs via the FcR, it is to a lesser degree [14–16,48]. FDCs can acquire antigen through various pathways, including direct interaction by small antigens as well as by binding to complement component 3 (C3) fragments on ICs via CR2/CR1 when presented to them via B cells [17,48]. It has been previously described that C3 fragments, specifically C3d, could therefore be used as a vaccine adjuvant [49]. A study by Ross et al. demonstrated the effectiveness of C3d-fusions to Influenza virus haemagglutinin in enhancing antibody production and maturation, leading to a protective immune response in the influenza mouse model [50]. This would be a particularly interesting area of research for FMDV, due to the short duration of immunity after FMD vaccination. If fusion of C3d to FMD vaccine antigens resulted in targeted antigen deposition on FDCs, this could improve the magnitude and duration of the neutralising antibody response.

Similar to other studies with FMDV [31], we have been unable to demonstrate that FMDV retained by FDCs in mice is infectious. Furthermore, in cattle persistently infected with FMDV, viral non-structural proteins associated with viral replication were not detected in the GC-containing regions of lymphoid tissues, therefore suggesting that persisting FMDV antigen, likely associated to FDCs, is non-replicative [24]. Bachmann et al. reported similar findings with VSV, that whilst VSV was not infectious on FDCs, the long duration of immunity seen was possible due to FDCs trapping and retaining antigen for long periods of time [20]. Therefore, despite the presence of FMDV on FDCs for long periods of time, this is in a non-infectious form, thus indicating a potential for non-infectious vaccines to reproduce this persistence to enhance the duration of immunity by eliciting FMDV-specific antibodies without the need for infectious virus.

Although the current study has highlighted the role of FDCs in the maintenance of neutralising antibodies to FMDV, further experiments are required to delineate GC and extrafollicular responses in order to understand how FMDV persistence results in the generation and

maintenance of the specific immune response in greater detail. Studies have shown that low-affinity plasmablasts are produced in transient primary extrafollicular foci, prior to somatic hypermutation and affinity maturation in GCs [51–54]. Therefore, up to 7 dpi the lack of significant differences in the results between 4B2 treated and control mice could be because of an extracellular, GC-independent response in both groups, which would also explain the low avidity of antibodies to the FMD capsid as shown by BLI. Although Ig class switching occurs extrafollicularly, there is evidence of only low-level hypermutation, thus the production of low affinity B cells in the initial stages of infection [55–57]. Consequently, the mAb 4B2 may have a lesser effect in the early stages of the adaptive immune response, where the GC reaction and FDCs are less involved. Furthermore, the similar titres of antibodies seen in both groups from 14 dpi could indicate a long-term extrafollicular response in the mAb 4B2 treated group, where plasma cells are produced, but the affinity maturation process is less effective than in the GC, which is then reflected in the lower avidity antibodies produced in mice treated with mAb 4B2 compared to the control mice. A review by Elsner et al. highlighted potential factors which could be studied to help understand the FMDV GC and extrafollicular responses in more detail [58]. For example, interleukin (IL)-12 has been shown to block T follicular helper cells (Tfh) and suppress GCs, resulting in an extrafollicular dominant response. Whereas, IL-6 promotes early GC reactions by promoting Tfh and blocking Th1.

Our study provides new insight into the immune pathogenesis of FMDV by demonstrating the interaction of the virus with FDCs. Studies in cattle and African buffalo have shown the virus localises to GC-containing regions of lymphoid tissues after the resolution of acute infection, but now we have demonstrated that FMDV binds as an IC to FDCs via CR2/CR1 in mice. We have also shown this interaction is crucial for the production of high avidity neutralising antibodies after FMDV infection. Furthermore, when CR2/CR1 is blocked, there is a significant reduction in the avidity of antibodies and a significant reduction in FMDV neutralising responses in serum. Short duration of immunity is one of the major problems with current killed FMDV vaccines, these studies provide insights into how the duration of protective antibody responses may be increased post-vaccination.

Materials and methods

Ethics statement

All animal experiments were performed in the animal isolation facilities at the Pirbright institute and were conducted in compliance with the Home Office Animals (scientific procedures) ACT 1986 and approved by the Pirbright Institute's Animal Welfare and Ethical Review Board (AWERB).

Mice and experiment design

Experiments were carried out to address 3 objectives; firstly, to determine whether the mAb 4B2 successfully blocked CR2/CR1 by using PAP which is known to bind to FDCs via the CR2/CR1. Secondly, to determine the effect of 4B2 on the cell subsets of the spleen. Finally, a challenge study to determine whether FMDV needs to bind to FDCs via the CR2/CR1 to maintain a neutralising antibody response. Female BALB/c mice (8–12 weeks) were used in these experiments and were purchased from Charles River Laboratories, UK. Mice were acclimatised for 7 days before being used in experiments and were maintained with food and water ad-libitum and full environmental enrichment. Mice were humanely culled using isoflurane and a rising concentration of carbon dioxide (CO_2) method. Naïve mice were used as negative controls throughout the study and remained untreated and were not infected with FMDV.

4B2 treatment. BALB/c mice were given a single intraperitoneal (i.p.) injection of 200 μl of 0.5 mg purified mAb 4B2 to mouse CR2/CR1 (32). Animals treated with the same dose of a mAb anti-OVA IgG1, F2.3.58 antibody (2B Scientific, UK) were used as isotype matched controls. Two mice treated with 4B2 and two with the IgG1 control mAb were culled at 2- and 7-days post treatment "early time points", and a further two from each group at 22- and 35-days post treatment "late time points" to assess the effects of 4B2 on spleen cell subsets. The spleen samples were collected in RPMI media (Gibco, UK) and immediately processed in the lab for flow cytometry.

PAP treatment. To test the ability of 4B2 to block CR2/CR1 *in vivo*, mice were given a single injection of 100μl preformed rabbit peroxidase-anti-peroxidase (PAP) immune complexes (Sigma) intravenously 1 day after treatment with 4B2 (n = 4) or anti-OVA IgG1 (n = 4). Mice were culled 1 day later, and their spleens were collected in optimal cutting temperature (OCT) compound (VWR Chemicals, UK) and stored at -80˚ C to test for the presence of FDC-associated IC by confocal microscopy.

FMDV infection. 1 day after treatment with mAbs 4B2 or IgG1, mice were inoculated i.p. with a total dose of $10^{6.2}$ $TCID_{50}$ of FMDV/O/UKG/34/2001 in 200μl. After challenge, mice were bled from the tail vein at 2, 7, 14, 21 and 28 dpi. Terminal bleeding after culling from cardiac puncture and spleens from culled mice were collected from 8 animals at 7, 14, 21 and 28 dpi from each treatment group. The spleens were cut in half, with half collected in OCT for analysis by confocal microscopy and half collected in RPMI medium (Gibco, UK) for analysis by PCR. The whole blood samples were stored at 4˚ C overnight to allow blood clotting, the samples were centrifuged, and the serum was collected and stored at -80˚ C.

FMDV immune complex deposition

Spleens from naïve BALB/c mice embedded in OCT compound were cut using a cryostat (7–9 μm) and sections mounted on a superfrost slides. The samples were blocked with 5% normal goat serum (NGS) (abcam, UK) for 30 minutes prior to addition of ICs and controls. The FMDV ICs consisted of inactivated O1/Manisa/TUR/69 FMDV vaccine antigen and IBII FMDV O antibody at 1:1 ratio and incubated with NMS, providing the necessary complement, for 30 minutes. The controls were O1/Manisa/TUR/69 antigen or IBII FMDV O antibody with only the addition of complement in the form of NMS. The ICs and controls were diluted in PBS 1:10, resulting in a final concentration of 5% NMS, and added to the tissue sections for 1 hour at room temperature. The slides were washed and fixed with fixed with 4% paraformaldehyde for 20 minutes. A polyclonal rabbit anti-O FMDV was added to the slides for 1 hour at room temperature to detect FMDV ICs bound to the cryosections. The slides were washed and 4 μg/ml goat anti-rabbit IgG (H+L) cross-adsorbed secondary antibody, Alexa Fluor 488 (Invitrogen) was added for 1 hour at room temperature in the dark. The sections were counterstained with DAPI to distinguish cell nuclei. Spleen sections were visualised, imaged and all data was collected using a Leica SP8 confocal microscope (Leica Microsystems GmbH, Germany).

Processing splenocytes

The spleen samples collected in RPMI medium were homogenised and passed through 70 μm cell mesh strainers (BD Biosciences, UK). Cells were washed in RPMI medium by centrifugation and red blood cells were lysed with ACK lysing buffer (Sigma-Aldrich, UK). Following lysis, cells were washed twice in RPMI by centrifugation and re-suspended in RPMI complete medium (RPMI with 10% foetal bovine serum (Gibco, UK), 1% Gibco penicillin-streptomycin (10,000 U/ml) (Life Technologies, UK) and 1% Gibco MEM non-essential amino acids (100X)

(Life Technologies, UK)), counted and stored at 4˚ C overnight prior to flow cytometric analysis.

Flow cytometry

The processed splenocytes were distributed at 1 x 10^6 per well into Nunc 96-well round bottom microwell plates (Thermo Scientific, UK). The cells were blocked by adding 5μg/ml purified rat anti-mouse CD16/CD32 (mouse BD Fc Block) clone: 2.4G2 (BD Biosciences, UK) in autoMACS buffer (Miltenyi Biotec, UK). Cells were stained with CD8a-FITC (Life Technologies), CD4-PE (Miltenyi Biotec) to detect cytotoxic and helper T cells respectively and B220 biotin RA3-6B2 Alexa Fluor 647 to detect B cells (CD45R), CD11b-APC to detect dendritic cells and CD169 (Siglec-1)-APC to detect marginal zone macrophages. Streptavidin Molecular Probe Alexa-Fluor-633 conjugated secondary mAb (1μg/ml) (Invitrogen) was used to detect biotinylated antibodies 7E9 (BioLegend, UK) and 7G6 (BD Biosciences, UK) to identify CD21/CD35 (CR2/CR1) and 8C12 (BD Biosciences, UK) to identify CD35 (CR1). Single staining controls and no staining controls were also included for compensation purposes. The cells were then fixed with 1% paraformaldehyde, washed and resuspended in MACS buffer, before being read on the MACS Quant (Miltenyi Biotec, UK). The analysis was completed using FCS Express (De Novo Software, US).

Quantification of viraemia by plaque assay

Foetal goat tongue cells (ZZR cells), which are highly susceptible to FMDV, were grown up to 95–100% confluency in 6 well plates. Cells were washed in PBS and a 10-fold dilution of serum samples from 2 dpi (n = 30 and n = 22 from 4B2 and IgG1 treatment group, respectively) and 7 dpi (n = 4 per treatment group) were added to the wells. Serum from 2 naïve animals at 2 dpi and 1 naïve animal at 7 dpi were used as negative controls. Plates were incubated for 30 minutes at 37˚C with 5% CO_2 and then 3ml/well of Eagle's Overlay-Agarose (Eagle's overlay media (TPI, UK) and 2% agarose (Sigma, UK)) was added and allowed to set at room temperature. Plates were incubated at 37˚C with 5% CO_2 for 48 hours. Following incubation, plates were fixed, and plaques visualized by staining the cell monolayer with methylene blue in 4% formaldehyde in PBS for 24 hours at room temperature. The plates were washed with water and the agarose plugs discarded. The viraemia was expressed as the Log10 of the number of plaque forming units per ml (PFU/ml).

One Step RT-qPCR of serum samples

Due to low volumes of serum collected from the tail vein, serum samples from animals taken at 2 dpi were pooled to reach 50 μl. Therefore, FMDV genome copy number was measured by RT-qPCR in 6 pools of serum from IgG1 and 4B2 treated mice and 3 pools from the naïve groups. Fifty μl of serum samples taken from terminal bleeds from culled animals at 7 dpi were also analysed. The RNA was extracted using the MagVet Universal Isolation Kit (Thermo Fisher Scientific, UK) and the KingFisher Flex (Thermo Fisher Scientific, UK). The PCR was performed, using the SuperScript III Platinum One-Step Callahan 3D quantitative RT- qPCR, according to the standard protocol of the World Referenced Laboratory for FMDV, with a cut-off cycle threshold (Ct) of $\geq$ 35 [59]. Results were expressed as Log10 FMDV genome copy number (GCN)/ml of sample by extrapolating the Ct values to GCN by using a linear regression model with serial dilutions of in vitro synthetized 3D RNA standard.

RT-qPCR from tissues

Spleen samples were homogenised in 200 μl DMEM media (Gibco, UK) using the FastPrep-24 and lysing matrix tubes (MP Biomedicals) prior to RNA extraction (as described above).

Following RNA extraction, cDNA was generated using TaqMan reverse transcription reagents (Applied Biosystems, UK,). The EXPRESS qPCR SuperMix Universal Kit (Invitrogen, UK) was used for real time-PCR and the PCR reactions for FMDV 3D were performed as previously described, with a cut-off Ct value of $\geq$ 35[59]. The 18S ribosomal RNA housekeeping gene was used for normalisation based on previously published primers [60,61]. The PCR reaction was performed on a Stratagene MX3005p quantitative PCR instrument (Stratagene, USA). Results were expressed as Log10 FMDV RNA copies/10^8 copies 18S.

Immunofluorescence by confocal microscopy

The frozen spleens embedded in OCT compound were cut on a cryostat (7–9 μm), mounted on a superfrost slide and stored at -20˚ C overnight. The slides were air-dried, fixed with 4% paraformaldehyde and blocked with 5% NGS (abcam, UK). FDC networks visualised by staining with 1μg/ml Alexa Fluor 594-conjugated anti-mouse CD21/CD35 (CR2/CR1) antibody, clone 7E9 (BioLegend, UK), marginal zone macrophages were visualised using 1μg/ml CD169 (Siglec-1), clone MOMA-1 (Bio-Rad, UK), 2 μg/ml biotinylated llama single domain anti-FMDV 12S antibody VHH-M3 (Kindly provided by Dr M Harmsen, Central Veterinary Institute of Wageningen, AB Lelystad, The Netherlands) [62] was used to detect FMDV/O/UKG/34/2001 and goat anti-rabbit Molecular Probe Alexa-Fluor-488 was used to detect PAP IC. Goat anti-rat and streptavidin Molecular Probes Alexa-Fluor-488 and 633 conjugated secondary mAbs (Invitrogen) were used at 2 μg/ml and all sections were counterstained with DAPI to distinguish cell nuclei. Spleen sections were visualised, imaged and all data was collected using a Leica SP8 confocal microscope (Leica Microsystems GmbH, Germany).

The same protocol was used for the stimulated emission depletion (STED) with the following changes: goat anti-rat and streptavidin Molecular Probes Alexa-Fluor-488 and 555 conjugated secondary mAbs (Invitrogen) were used at 4 μg/ml, ToPro3 was used for nuclear staining and a super-resolution Leica TCS SP8 STED 3X microscope (Leica Microsystems GmbH, Germany) equipped with 592 and 660nm depletion lasers was used to image and collect data. STED images were then deconvolved in Huygens Professional software 21.04 (Scientific Volume Imaging, Netherlands) using the Deconvolution Wizard with a theoretical PSF. Data was analysed using ImageJ software as previously described [33,34] to compare the null hypothesis (that the pixels were randomly distributed) to the observed levels of co-localisation.

Virus isolation

Virus isolation was carried out to determine whether FMDV persisting in the murine spleens was infectious. Spleens were homogenised using FastPrep Lysing Matrix D tubes with the FastPrep-24 (MP Biomedicals). The spleen homogenate was then added to T25 flasks containing ZZR cells (goat tongue epithelial cells), which are susceptible to FMDV. The cells and homogenate were incubated at 37˚C in 5% CO2 and checked daily for cytopathic effect (CPE). After 48 hours the flasks were stores at -20˚C, and once frozen were defrosted, centrifuged and supernatant was collected. The supernatant from each sample was then added to new flasks of confluent ZZR cells and the process was repeated for a total of 3 passages. The presence of CPEs would demonstrate that the FMDV was infectious, absence of CPEs would demonstrate no infectious FMDV. A flask inoculated with FMDV-OUKG and a flask of ZZR cells only were used as positive and negative controls respectively for each passage.

Virus neutralising test

Serum samples collected at 7, 14, 21 and 28 dpi were heated at 56˚ C for 1 hour to inactivate complement and analysed for their ability to neutralise a fixed dose of FMDV on IB-RS-2 cells

porcine cells). Samples were then diluted 2-fold in 96 well plates in duplicate in serum free medium starting from a 1:8 dilution. Naïve mouse serum and cells only were used as negative controls. One hundred tissue culture infectious dose 50 ($TCID_{50}$) of FMDV OUKG was added to all wells excluding cell only controls. Plates were incubated for 1 hour at room temperature before 5×10^4 IB-RS-2 cells were dispensed to each well. The plates were incubated at 37˚C in 5% CO2 and checked daily for cytopathic effect (CPE). After 72 hours the plates were inactivated with 1% Trichloroacetic acid (TCA) (Sigma-Aldrich, UK) washed with water and stained with methylene blue. Neutralising antibody titre was calculated using the Spearmann-Karber formula and results expressed as the log_{10} reciprocal serum dilution that neutralised 50% of 100 $TCID_{50}$ of the virus [63].

IgG and IgM ELISA

An indirect enzyme-linked immunosorbent assay (ELISA) was developed to detect FMDV-specific mouse antibodies. The assay was adapted from the FMDV isotype specific ELISA protocol to detect antibodies to FMDV in cattle and swine serum [11]. ELISA plates were coated with a rabbit anti-O FMDV polyclonal antibody (TPI, UK), washed with PBS containing 0.05% Tween20 (Sigma, UK) and then 0.5 μg/ml inactivated FMDV O1/Manisa/TUR/69 vaccine antigen (Merial, UK), diluted in blocking buffer (1:1 PBS and SEA BLOCK (Thermo Scientific, UK)), was added to each well. Serum samples were added, and bound antibodies were detected by incubating the plates with horseradish peroxidase-conjugated goat anti-mouse IgG or IgM (Invitrogen, UK), diluted in blocking buffer. TMB substrate (Thermo Scientific, UK) was used as a developer and the reaction was stopped with 0.3M H_2SO_4 and the optical density (OD) was read at 450 nm. Antibody titres were expressed as either log10 of the reciprocal of the last dilution with a mean OD greater than 1.5 times the mean of the OD of the negative control serum or using an FMDV-specific IgG standard (IB11 mAb [11]) of known concentration, a standard curve was generated to determine the concentration of the FMDV-specific IgG in the serum samples analysed. The O1/Manisa/TUR/69 vaccine antigen was used due to good cross-reactivity and cross-protection with OUKG as demonstrated in previous studies [64–66].

Peptide ELISA

An indirect peptide ELISA using a biotinylated O/UKG/12/2001 G-H loop peptide (VYNGNCKYGESPVTNVRGDLQVLAQKAARTLPTSFNYGAIK) (Peptide Protein Research Ltd, UK) was developed to determine the presence of antibodies directed against the FMDV $VP1_{129\text{-}169}$ G-H loop. The highest concentration of each serum sample was also tested with a biotinylated negative control peptide with a similar molecular weight and number of charged residues vs hydrophobic residues (PSRDYSHYYTTIQDLRDKILGATIENSRIVLQIDNARLA) (Peptide Protein Research Ltd, UK) to ensure the sera wasn't binding non-specifically. Streptavidin coated ELISA plates (Thermo Scientific) were incubated with 8 μg/ml G-H loop peptide diluted in PBS at 37˚C for 2 hours. The plates were washed with TBS containing 0.1% BSA 0.05% Tween20 (Sigma, UK) and then serum samples were added in duplicate. Bound antibodies were detected by horseradish peroxidase-conjugated goat anti-mouse IgG (Invitrogen, UK) and SIGMAFAST OPD (o-Phenylenediamine dihydrochloride) (Sigma, UK). The optical densities (OD) were measured at 450nm, and antibody titres were expressed as log10 of the reciprocal of the last dilution with a mean OD greater than 1.5 times the mean of the OD of the negative control serum.

Biolayer interferometry

Biolayer interferometry was performed using an Octet Red96e instrument (ForteBio, Inc.) and ForteBio Data Analysis HT software (v 11.1.0.25) was used to determine the response rate,

k_{off}/k_{on} rates and the K_D (M) values. This method was adapted from previously described methods using polyclonal sera [67,68]. A 5 μg/ml concentration of biotinylated stable O1/Manisa/TUR/69 FMD VLP [69] (kindly provided by Alison Burman) was immobilised on streptavidin-coated biosensors (Sartorius UK Limited) for 900 s. A baseline was established by measurements taken when sensors were immersed for 60 s in HEPES 10 mM, NaCl 150 mM, EDTA 3 mM, 0.005% Tween 20 (HBS-EP) buffer (Teknova). The sensors were then immersed in a dilution series of polyclonal sera, with known FMDV-specific IgG concentrations, from mice taken at 7, 14 or 21 dpi with FMDV for 1200 s in the association phase. Subsequently, the sensors were immersed in HBS-EP buffer for 1200 s in the dissociation phase. Unloaded sensors and reference wells were used to subtract non-specific binding. Mean K_D (M) values were obtained from the dilution series of each mouse based on their global fit to a bivalent model, with a full R^2 value of $\geq$0.9. The K_D values were measured using the ratio of k_{off}/k_{on}, to determine the avidity of antibodies in the polyclonal serum samples to the FMD VLP. The values were expressed as -Log10 of K_D (M) values, and sera which had a response rate below 0 were recorded as 0.

Statistical analysis

The comparisons between the experimental groups and their corresponding control groups were carried out using Minitab software (Minitab, US). The non-parametric Mann-Whitney *U* test was used to compare the medians of viremia, presence of antigen, antibody titres and avidities and splenic cell subsets between the 4B2 and IgG1 treated groups. A *P* value of ≤ 0.05 was considered statistically significant.

Supporting information

S1 Table. A summary list of the animals used in the *in vivo* CR2/CR1-blockade experiment and their corresponding results.
(XLSX)

Acknowledgments

We thank The Pirbright Institute animal services team, in particular David Selby, for their help with the *in vivo* procedures; Andrew Shaw and Holly Everest (The Pirbright Institute) for their guidance with the Octet; Barry Bradford (The Roslin Institute, University of Edinburgh) for his help with ImageJ; the bioimaging team (The Pirbright Institute), namely Jennifer Simpson and the flow cytometry facility (The Pirbright Institute).

Author Contributions

Conceptualization: Lucy Gordon, Neil Mabbott, Nick Juleff, Bryan Charleston, Eva Perez-Martin.

Data curation: Lucy Gordon.

Formal analysis: Lucy Gordon, Eva Perez-Martin.

Funding acquisition: Neil Mabbott, Bryan Charleston.

Investigation: Lucy Gordon, Joanna Wells.

Methodology: Lucy Gordon, Eva Perez-Martin.

Resources: Neil Mabbott, Liudmila Kulik.

Supervision: Neil Mabbott, Bryan Charleston, Eva Perez-Martin.

Visualization: Joanna Wells.

Writing – original draft: Lucy Gordon, Bryan Charleston.

Writing – review & editing: Lucy Gordon, Neil Mabbott, Liudmila Kulik, Nick Juleff, Eva Perez-Martin.

References

1. Alexandersen S, Zhang Z, Donaldson AI. Aspects of the persistence of foot-and-mouth disease virus in animals—the carrier problem. Microbes Infect. 2002; 4(10):1099–110. https://doi.org/10.1016/s1286-4579(02)01634-9 PMID: 12191660
2. Arzt J, Belsham GJ, Lohse L, Botner A, Stenfeldt C. Transmission of Foot-and-Mouth Disease from Persistently Infected Carrier Cattle to Naive Cattle via Transfer of Oropharyngeal Fluid. mSphere. 2018; 3 (5):e00365–18. https://doi.org/10.1128/mSphere.00365-18 PMID: 30209130
3. Sutmoller P, Gaggero A. Foot-and mouth diseases carriers. Vet Rec. 1965; 77(33):968–9. https://doi.org/10.1136/vr.77.33.968 PMID: 5890082
4. Condy JB, Hedger RS, Hamblin C, Barnett IT. The duration of the foot-and-mouth disease virus carrier state in African buffalo (i) in the individual animal and (ii) in a free-living herd. Comp Immunol Microbiol Infect Dis. 1985; 8(3–4):259–65. https://doi.org/10.1016/0147-9571(85)90004-9 PMID: 3004803
5. Hedger RS. Foot-and-mouth disease and the African buffalo (Syncerus caffer). J Comp Pathol. 1972; 82(1):19–28. https://doi.org/10.1016/0021-9975(72)90022-9 PMID: 4336115
6. Alexandersen S, Zhang Z, Donaldson AI, Garland AJ. The pathogenesis and diagnosis of foot-and-mouth disease. J Comp Pathol. 2003; 129(1):1–36. https://doi.org/10.1016/s0021-9975(03)00041-0 PMID: 12859905
7. Jolles A, Gorsich E, Gubbins S, Beechler B, Buss P, Juleff N, et al. Endemic persistence of a highly contagious pathogen: Foot-and-mouth disease in its wildlife host. Science. 2021; 374(6563):104–9. https://doi.org/10.1126/science.abd2475 PMID: 34591637
8. Anderson EC, Doughty WJ, Anderson J, Paling R. The pathogenesis of foot-and-mouth disease in the African buffalo (Syncerus caffer) and the role of this species in the epidemiology of the disease in Kenya. J Comp Pathol. 1979; 89(4):541–9. https://doi.org/10.1016/0021-9975(79)90045-8 PMID: 232107
9. Stenfeldt C, Eschbaumer M, Rekant SI, Pacheco JM, Smoliga GR, Hartwig EJ, et al. The Foot-and-Mouth Disease Carrier State Divergence in Cattle. J Virol. 2016; 90(14):6344–64. https://doi.org/10.1128/JVI.00388-16 PMID: 27147736
10. Cunliffe HR. Observations on the Duration of Immunity in Cattle after Experimental Infection with Foot-and-Mouth Disease Virus. Cornell Vet. 1964; 54:501–10. PMID: 14234053
11. Juleff N, Windsor M, Lefevre EA, Gubbins S, Hamblin P, Reid E, et al. Foot-and-mouth disease virus can induce a specific and rapid CD4+ T-cell-independent neutralizing and isotype class-switched antibody response in naive cattle. J Virol. 2009; 83(8):3626–36. https://doi.org/10.1128/JVI.02613-08 PMID: 19176618
12. Carr BV, Lefevre EA, Windsor MA, Inghese C, Gubbins S, Prentice H, et al. CD4+ T-cell responses to foot-and-mouth disease virus in vaccinated cattle. J Gen Virol. 2013; 94(Pt 1):97–107. https://doi.org/10.1099/vir.0.045732-0 PMID: 23034593
13. Grant CFJ, Carr BV, Singanallur NB, Morris J, Gubbins S, Hudelet P, et al. The B-cell response to foot-and-mouth-disease virus in cattle following vaccination and live-virus challenge. J Gen Virol. 2016; 97 (9):2201–9. https://doi.org/10.1099/jgv.0.000517 PMID: 27260141
14. Heesters BA, Chatterjee P, Kim YA, Gonzalez SF, Kuligowski MP, Kirchhausen T, et al. Endocytosis and recycling of immune complexes by follicular dendritic cells enhances B cell antigen binding and activation. Immunity. 2013; 38(6):1164–75. https://doi.org/10.1016/j.immuni.2013.02.023 PMID: 23770227
15. Carroll MC. The role of complement and complement receptors in induction and regulation of immunity. Annu Rev Immunol. 1998; 16(1):545–68.
16. Imal Y, Yamakawa M. Morphology, function and pathology of follicular dendritic cells. Pathol Int. 1996; 46(11):807–33. https://doi.org/10.1111/j.1440-1827.1996.tb03555.x PMID: 8970191
17. Heesters BA, Myers RC, Carroll MC. Follicular dendritic cells: dynamic antigen libraries. Nat Rev Immunol. 2014; 14(7):495–504. https://doi.org/10.1038/nri3689 PMID: 24948364

18. Aguzzi A, Kranich J, Krautler NJ. Follicular dendritic cells: origin, phenotype, and function in health and disease. Trends Immunol. 2014; 35(3):105–13. https://doi.org/10.1016/j.it.2013.11.001 PMID: 24315719

19. Carroll MC. Complement and humoral immunity. Vaccine. 2008; 26 Suppl 8(0 8):I28–33. https://doi.org/10.1016/j.vaccine.2008.11.022 PMID: 19388161

20. Bachmann MF, Odermatt B, Hengartner H, Zinkernagel RM. Induction of long-lived germinal centers associated with persisting antigen after viral infection. J Exp Med. 1996; 183(5):2259–69. https://doi.org/10.1084/jem.183.5.2259 PMID: 8642335

21. Fray MD, Supple EA, Morrison WI, Charleston B. Germinal centre localization of bovine viral diarrhoea virus in persistently infected animals. J Gen Virol. 2000; 81(Pt 7):1669–73. https://doi.org/10.1099/0022-1317-81-7-1669 PMID: 10859371

22. McCulloch L, Brown KL, Bradford BM, Hopkins J, Bailey M, Rajewsky K, et al. Follicular Dendritic Cell-Specific Prion Protein (PrPc) Expression Alone Is Sufficient to Sustain Prion Infection in the Spleen. Plos Pathogens. 2011; 7(12). https://doi.org/10.1371/journal.ppat.1002402 PMID: 22144895

23. Heesters BA, Lindqvist M, Vagefi PA, Scully EP, Schildberg FA, Altfeld M, et al. Follicular Dendritic Cells Retain Infectious HIV in Cycling Endosomes. PLoS Pathog. 2015; 11(12):e1005285. https://doi.org/10.1371/journal.ppat.1005285 PMID: 26623655

24. Juleff N, Windsor M, Reid E, Seago J, Zhang Z, Monaghan P, et al. Foot-and-mouth disease virus persists in the light zone of germinal centres. Plos One. 2008; 3(10):e3434. https://doi.org/10.1371/journal.pone.0003434 PMID: 18941503

25. Stenfeldt C, Hartwig EJ, Smoliga GR, Palinski R, Silva EB, Bertram MR, et al. Contact Challenge of Cattle with Foot-and-Mouth Disease Virus Validates the Role of the Nasopharyngeal Epithelium as the Site of Primary and Persistent Infection. mSphere. 2018; 3(6):e00493–18. https://doi.org/10.1128/mSphere.00493-18 PMID: 30541776

26. Maree F, de Klerk-Lorist LM, Gubbins S, Zhang F, Seago J, Perez-Martin E, et al. Differential Persistence of Foot-and-Mouth Disease Virus in African Buffalo Is Related to Virus Virulence. J Virol. 2016; 90(10):5132–40. https://doi.org/10.1128/JVI.00166-16 PMID: 26962214

27. Mabbott NA, Bruce ME, Botto M, Walport MJ, Pepys MB. Temporary depletion of complement component C3 or genetic deficiency of C1q significantly delays onset of scrapie. Nat Med. 2001; 7(4):485–7. https://doi.org/10.1038/86562 PMID: 11283677

28. Klein MA, Kaeser PS, Schwarz P, Weyd H, Xenarios I, Zinkernagel RM, et al. Complement facilitates early prion pathogenesis. Nat Med. 2001; 7(4):488–92. https://doi.org/10.1038/86567 PMID: 11283678

29. Ho J, Moir S, Kulik L, Malaspina A, Donoghue ET, Miller NJ, et al. Role for CD21 in the establishment of an extracellular HIV reservoir in lymphoid tissues. J Immunol. 2007; 178(11):6968–74. https://doi.org/10.4049/jimmunol.178.11.6968 PMID: 17513746

30. Habiela M, Seago J, Perez-Martin E, Waters R, Windsor M, Salguero FJ, et al. Laboratory animal models to study foot-and-mouth disease: a review with emphasis on natural and vaccine-induced immunity. J Gen Virol. 2014; 95(Pt 11):2329–45. https://doi.org/10.1099/vir.0.068270-0 PMID: 25000962

31. Doudo MHA. THE ROLE OF FOLLICULAR DENDRITIC CELLS AND PERSISTING FOOT-AND-MOUTH DISEASE VIRUS ANTIGENS AS DETERMINANTS OF IMMUNE RESPONSES TO THE VIRUS: University of Cambridge; 2017.

32. Kulik L, Hewitt FB, Willis VC, Rodriguez R, Tomlinson S, Holers VM. A new mouse anti-mouse complement receptor type 2 and 1 (CR2/CR1) monoclonal antibody as a tool to study receptor involvement in chronic models of immune responses and disease. Mol Immunol. 2015; 63(2):479–88. https://doi.org/10.1016/j.molimm.2014.10.005 PMID: 25457881

33. McCulloch L, Brown KL, Bradford BM, Hopkins J, Bailey M, Rajewsky K, et al. Follicular dendritic cell-specific prion protein (PrP) expression alone is sufficient to sustain prion infection in the spleen. PLoS Pathog. 2011; 7(12):e1002402. https://doi.org/10.1371/journal.ppat.1002402 PMID: 22144895

34. Inman CF, Rees LE, Barker E, Haverson K, Stokes CR, Bailey M. Validation of computer-assisted, pixel-based analysis of multiple-colour immunofluorescence histology. J Immunol Methods. 2005; 302(1–2):156–67. https://doi.org/10.1016/j.jim.2005.05.005 PMID: 15992812

35. Victoratos P, Lagnel J, Tzima S, Alimzhanov MB, Rajewsky K, Pasparakis M, et al. FDC-specific functions of p55TNFR and IKK2 in the development of FDC networks and of antibody responses. Immunity. 2006; 24(1):65–77. https://doi.org/10.1016/j.immuni.2005.11.013 PMID: 16413924

36. Zamorano P, Wigdorovitz A, Perez-Filgueira M, Carrillo C, Escribano JM, Sadir AM, et al. A 10-amino-acid linear sequence of VP1 of foot and mouth disease virus containing B- and T-cell epitopes induces protection in mice. Virology. 1995; 212(2):614–21. https://doi.org/10.1006/viro.1995.1519 PMID: 7571431

37. Rodriguez LL, Barrera J, Kramer E, Lubroth J, Brown F, Golde WT. A synthetic peptide containing the consensus sequence of the G-H loop region of foot-and-mouth disease virus type-O VP1 and a promiscuous T-helper epitope induces peptide-specific antibodies but fails to protect cattle against viral challenge. Vaccine. 2003; 21(25–26):3751–6. https://doi.org/10.1016/s0264-410x(03)00364-5 PMID: 12922108

38. Qin D, Wu J, Vora KA, Ravetch JV, Szakal AK, Manser T, et al. Fc gamma receptor IIB on follicular dendritic cells regulates the B cell recall response. J Immunol. 2000; 164(12):6268–75. https://doi.org/10.4049/jimmunol.164.12.6268 PMID: 10843680

39. Ochsenbein AF, Pinschewer DD, Odermatt B, Carroll MC, Hengartner H, Zinkernagel RM. Protective T cell-independent antiviral antibody responses are dependent on complement. J Exp Med. 1999; 190 (8):1165–74. https://doi.org/10.1084/jem.190.8.1165 PMID: 10523614

40. Jacobson AC, Weis JH. Comparative functional evolution of human and mouse CR1 and CR2. J Immunol. 2008; 181(5):2953–9. https://doi.org/10.4049/jimmunol.181.5.2953 PMID: 18713965

41. Chen Z, Koralov SB, Gendelman M, Carroll MC, Kelsoe G. Humoral immune responses in Cr2-/- mice: enhanced affinity maturation but impaired antibody persistence. J Immunol. 2000; 164(9):4522–32. https://doi.org/10.4049/jimmunol.164.9.4522 PMID: 10779753

42. Molina H, Holers VM, Li B, Fung Y, Mariathasan S, Goellner J, et al. Markedly impaired humoral immune response in mice deficient in complement receptors 1 and 2. Proc Natl Acad Sci U S A. 1996; 93(8):3357–61. https://doi.org/10.1073/pnas.93.8.3357 PMID: 8622941

43. Anania JC, Westin A, Adler J, Heyman B. A Novel Image Analysis Approach Reveals a Role for Complement Receptors 1 and 2 in Follicular Dendritic Cell Organization in Germinal Centers. Front Immunol. 2021; 12(1136):655753. https://doi.org/10.3389/fimmu.2021.655753 PMID: 33912182

44. Pikor NB, Morbe U, Lutge M, Gil-Cruz C, Perez-Shibayama C, Novkovic M, et al. Remodeling of light and dark zone follicular dendritic cells governs germinal center responses. Nat Immunol. 2020; 21 (6):649–59. https://doi.org/10.1038/s41590-020-0672-y PMID: 32424359

45. Ahearn JM, Fischer MB, Croix D, Goerg S, Ma M, Xia J, et al. Disruption of the Cr2 locus results in a reduction in B-1a cells and in an impaired B cell response to T-dependent antigen. Immunity. 1996; 4 (3):251–62. https://doi.org/10.1016/s1074-7613(00)80433-1 PMID: 8624815

46. Barrington RA, Pozdnyakova O, Zafari MR, Benjamin CD, Carroll MC. B lymphocyte memory: role of stromal cell complement and FcgammaRIIB receptors. J Exp Med. 2002; 196(9):1189–99. https://doi.org/10.1084/jem.20021110 PMID: 12417629

47. Fang YF, Xu CG, Fu YX, Holers VM, Molina H. Expression of complement receptors 1 and 2 on follicular dendritic cells is necessary for the generation of a strong antigen-specific IgG response. J Immunol. 1998; 160(11):5273–9. PMID: 9605124

48. Nielsen CH, Fischer EM, Leslie RG. The role of complement in the acquired immune response. Immunology. 2000; 100(1):4–12. https://doi.org/10.1046/j.1365-2567.2000.00009.x PMID: 10809953

49. Dempsey PW, Allison ME, Akkaraju S, Goodnow CC, Fearon DT. C3d of complement as a molecular adjuvant: bridging innate and acquired immunity. Science. 1996; 271(5247):348–50. https://doi.org/10.1126/science.271.5247.348 PMID: 8553069

50. Ross TM, Xu Y, Bright RA, Robinson HL. C3d enhancement of antibodies to hemagglutinin accelerates protection against influenza virus challenge. Nat Immunol. 2000; 1(2):127–31. https://doi.org/10.1038/77802 PMID: 11248804

51. Smith KGC, Hewitson TD, Nossal GJV, Tarlinton DM. The phenotype and fate of the antibody-forming cells of the splenic foci. Eur J Immunol. 1996; 26(2):444–8. https://doi.org/10.1002/eji.1830260226 PMID: 8617316

52. Dal Porto JM, Haberman AM, Shlomchik MJ, Kelsoe G. Antigen Drives Very Low Affinity B Cells to Become Plasmacytes and Enter Germinal Centers. J Immunol. 1998; 161(10):5373–81. PMID: 9820511

53. Phan TG, Paus D, Chan TD, Turner ML, Nutt SL, Basten A, et al. High affinity germinal center B cells are actively selected into the plasma cell compartment. J Exp Med. 2006; 203(11):2419–24. https://doi.org/10.1084/jem.20061254 PMID: 17030950

54. Fink K, Manjarrez-Orduño N, Schildknecht A, Weber J, Senn BM, Zinkernagel RM, et al. B Cell Activation State-Governed Formation of Germinal Centers following Viral Infection. J Immunol. 2007; 179 (9):5877–85. https://doi.org/10.4049/jimmunol.179.9.5877 PMID: 17947661

55. Smith KG, Light A, Nossal GJ, Tarlinton DM. The extent of affinity maturation differs between the memory and antibody-forming cell compartments in the primary immune response. EMBO J. 1997; 16 (11):2996–3006. https://doi.org/10.1093/emboj/16.11.2996 PMID: 9214617

56. MacLennan ICM, Toellner K-M, Cunningham AF, Serre K, Sze DM-Y, Zúñiga E, et al. Extrafollicular antibody responses. Immunol Rev. 2003; 194(1):8–18. https://doi.org/10.1034/j.1600-065x.2003.00058.x PMID: 12846803

57. Shlomchik MJ, Luo W, Weisel F. Linking signaling and selection in the germinal center. Immunol Rev. 2019; 288(1):49–63. https://doi.org/10.1111/imr.12744 PMID: 30874353

58. Elsner RA, Shlomchik MJ. Germinal Center and Extrafollicular B Cell Responses in Vaccination, Immunity, and Autoimmunity. Immunity. 2020; 53(6):1136–50. https://doi.org/10.1016/j.immuni.2020.11.006 PMID: 33326765

59. King DP, Ferris NP, Shaw AE, Reid SM, Hutchings GH, Giuffre AC, et al. Detection of foot-and-mouth disease virus: comparative diagnostic sensitivity of two independent real-time reverse transcription-polymerase chain reaction assays. J Vet Diagn Invest. 2006; 18(1):93–7. https://doi.org/10.1177/104063870601800114 PMID: 16566264

60. Proudnikov D, Yuferov V, Zhou Y, LaForge KS, Ho A, Kreek MJ. Optimizing primer—probe design for fluorescent PCR. J Neurosci Methods. 2003; 123(1):31–45. https://doi.org/10.1016/s0165-0270(02)00325-4 PMID: 12581847

61. Afonina IA, Mills A, Sanders S, Kulchenko A, Dempcy R, Lokhov S, et al. Improved biplex quantitative real-time polymerase chain reaction with modified primers for gene expression analysis. Oligonucleotides. 2006; 16(4):395–403. https://doi.org/10.1089/oli.2006.16.395 PMID: 17155914

62. Harmsen MM, Fijten HP, Westra DF, Coco-Martin JM. Effect of thiomersal on dissociation of intact (146S) foot-and-mouth disease virions into 12S particles as assessed by novel ELISAs specific for either 146S or 12S particles. Vaccine. 2011; 29(15):2682–90. https://doi.org/10.1016/j.vaccine.2011.01.069 PMID: 21316500

63. Kärber G. Beitrag zur kollektiven Behandlung pharmakologischer Reihenversuche. Naunyn-Schmiedebergs Archiv für Experimentelle Pathologie und Pharmakologie. 1931; 162(4):480–3.

64. Aggarwal N, Zhang Z, Cox S, Statham R, Alexandersen S, Kitching RP, et al. Experimental studies with foot-and-mouth disease virus, strain O, responsible for the 2001 epidemic in the United Kingdom. Vaccine. 2002; 20(19–20):2508–15. https://doi.org/10.1016/s0264-410x(02)00178-0 PMID: 12057606

65. Cox SJ, Voyce C, Parida S, Reid SM, Hamblin PA, Paton DJ, et al. Protection against direct-contact challenge following emergency FMD vaccination of cattle and the effect on virus excretion from the oropharynx. Vaccine. 2005; 23(9):1106–13. https://doi.org/10.1016/j.vaccine.2004.08.034 PMID: 15629353

66. Knowles NJ, Samuel AR, Davies PR, Midgley RJ, Valarcher JF. Pandemic strain of foot-and-mouth disease virus serotype O. Emerg Infect Dis. 2005; 11(12):1887–93. https://doi.org/10.3201/eid1112.050908 PMID: 16485475

67. Dennison SM, Reichartz M, Seaton KE, Dutta S, Wille-Reece U, Hill AVS, et al. Qualified Biolayer Interferometry Avidity Measurements Distinguish the Heterogeneity of Antibody Interactions with Plasmodium falciparum Circumsporozoite Protein Antigens. J Immunol. 2018; 201(4):1315–26. https://doi.org/10.4049/jimmunol.1800323 PMID: 30006374

68. Tsuji I, Dominguez D, Egan MA, Dean HJ. Development of a novel assay to assess the avidity of dengue virus-specific antibodies elicited in response to a tetravalent dengue vaccine. J Infect Dis. 2021. https://doi.org/10.1093/infdis/jiab064 PMID: 33534885

69. Porta C, Kotecha A, Burman A, Jackson T, Ren J, Loureiro S, et al. Rational engineering of recombinant picornavirus capsids to produce safe, protective vaccine antigen. PLoS Pathog. 2013; 9(3):e1003255. https://doi.org/10.1371/journal.ppat.1003255 PMID: 23544011